

GAS TURBINE INTERNAL BLADE COOLING STUDY

MOHD HAZRAN BIN MAT RAHIM

MECHANICAL ENGINEERING
UNIVERSITI TEKNOLOGI PETRONAS
DECEMBER 2010

CERTIFICATION OF APPROVAL

Gas Turbine Internal Blade Cooling Study

By

Mohd Hazran bin Mat Rahim

A project dissertation submitted to the

Mechanical Engineering Programme

Universiti Teknologi PETRONAS

in partial fulfilment of the requirement for the

BACHELOR OF ENGINEERING (Hons)

(MECHANICAL ENGINEERING)

Approved by,

(IR IDRIS BIN IBRAHIM)
UNIVERSITI TEKNOLOGI PETRONAS
TRONOH, PERAK

December 2010

CERTIFICATION OF ORIGINALITY

This is to certify that I am responsible for the work submitted in this project, that the original work is my own except as specified in the references and acknowledgements, and that the original work contained herein have not been undertaken or done by unspecified sources or persons.

MOHD HAZRAN BIN MAT RAHIM

ABSTRACT

Gas Turbine engine is the engine that converts the energy of the moving stream of fluid into mechanical energy. It consists of four stages of the following four processes which are compression, combustion, expansion and exhaust. In expansion stage, hot gas expands across the turbine rotors. In this stage, the power turbine blades after the combustion chamber are located at very high pressure and temperature condition. This condition can affect and damage the strength, material and structure of the power turbine blade. The purpose of the project is to investigate and analyze the temperature profile along the turbine blade surface and to study on the fluid flow and heat transfer distribution of the turbine blade during the internal cooling process. It is important to ensure proper cooling can be performed. The scopes of study of the project are modeling the turbine blade, simulation of the model using ANSYS and ANSYS FLUENT, validation using publishes data by excluding the physical experiment and sensitivity study to look on the effect of the number and size of the holes and also effect on the types of hole of the turbine blade in the simulation. This project is done into several stages of process. Research and data collection is conducted for the system and the design of the blade. Then, the design and analysis of the turbine blade is carried up with software such as CATIA, ANSYS and FLUENT. Once all the design and analysis meet the specification, the sensitivity study of the model is carried up to look on the effect of the number and size of the holes and also effect on the types of hole of the turbine blade. From the simulation and analysis, it is proves that the design with cooling channel affect the temperature distribution along the turbine blade. Then, the author observes the effect of the number and size of the holes and also effect on the types of hole of the turbine blade. From both of the sensitivity study, the results show the holes at the blade and increase of number of cooling channels will improve the efficiency of the engine better as the thermal growth along the blade is improved. That conclusion satisfied the gas turbine cooling concept.

ACKNOWLEDGEMENT

First and foremost, I would like to extend my utmost gratitude to Allah Almighty for ensuring successful flow of my Final Year Project (FYP). Then, I would like express my deep appreciation to my supervisor, Ir Idris Bin Ibrahim, Senior Lecturer, Mechanical Engineering Department, Universiti Teknologi PETRONAS, for guiding and supporting me with advices and concern throughout one year of doing this Final Year Project (FYP).

Besides, the special credit goes to Mr Mat Rahim bin Hussin and Madam Siti Zabidah binti Daud for their inspiration and word of wisdom which is putting me through all hurdles that led to this achievement. A special thanks to my siblings for their endless support and encouragement in accomplishing this project.

I also would like to forward my appreciation to UTP Graduate Assistant (GA) and my friends for their help to get me in better understanding of this project especially the procedure of using ANSYS software. Their help really help me in making this project a success.

Lastly, I would like to expand my appreciation to all lecturers who have helped and supported me directly or indirectly throughout this project. All their knowledge and experiences will be a great asset and guidance for my upcoming profession as an engineer.

TABLE OF CONTENT

CERTIFICATION	i
ABSTRACT	iii
ACKNOWLEDGEMENT	iv
CHAPTER 1: INTRODUCTION	1
1.1 Background of Study	1
1.2 Problem Statement	2
1.3 Objective	3
1.4 Scope of study	3
CHAPTER 2: LITERATURE REVIEW	4
2.1 Concept of Turbine Blade Cooling	4
2.2 Internal Gas Turbine Cooling Systems	5
2.3 Jet-Impingement Cooling	7
2.4 Rib-Turbulated Cooling	9
2.5 Pin-Fin Cooling	13
2.6 Design Geometry and Boundary Condition	16
2.7 Analysis and Expected Results	19
CHAPTER 3: METHODOLOGY / PROJECT WORK	23
3.1 Flowchart/Procedure of Project Development	23
3.2 Overview of the Methodology	24

CHAPTER 4:	RESULT & DISCUSSION	43
4.1	Base Model Fluid Flow/External Aerodynamics	43
4.2	Base Model Temperature Distribution/Thermal Analysis.	45
4.3	Turbine Blade Model with External and Pin-Fin Holes.	45
4.4	Turbine Blade Model with 9 Cooling Channels	43
CHAPTER 5:	CONCLUSION AND RECOMMENDATION.	52
REFERENCES		53
APPENDICES		54

LIST OF FIGURES

Figure 1.1	Brayton Cycle	1
Figure 2.1(a)	Figure 2: High pressure turbine rotor blade internally cooled for GE CF6 engine (Treager,1979)	5
Figure 2.1(b)	Typical cooled aircraft gas turbine blade (Gladden and Simoneau, 1988; collected in Sokolowski, 1989)	5
Figure 2.2	Cooling Concepts of a modern multi-pass turbine blade	6
Figure 2.3(a)	Schematic of the impingement cooling at the turbine blades leading edge (Chupp et., 1968)	7
Figure 2.3(b)	Flow regions caused by a jet impingement (Viskanta, 1993)	8
Figure 2.4(a)	Schematic Flow separation and rib orientations in heat-transfer coefficient enhancement (Han and Dutta ,1995)	10
Figure 2.4(b)	Typical coolant channels in the turbine blade and internal rib arrangement (Han, 1988)	11
Figure 2.5(a)	The trailing edge of the turbine blade is cooled by pin fins (Metzger et al., 1984)	13
Figure 2.5(b)	Four typical ejection hole configurations used by Lau et al. (1989a)	14
Figure 2.6(a)	NASA E ³ blade solid model and corresponding finite element ANSYS model	16
Figure 2.6(b)	Turbine blade design geometry	17
Figure 2.7(a)	NASA E ³ blade solid thermal results	19
Figure 2.7(b)	Total Pressure Contour Lines (Yellow color is vortex core, only lower half blade part is shown)	19
Figure 2.7(c)	Streamlines Surface and 3D secondary flow at hub	20
Figure 2.7(d)	Temperature distribution for the blade without cooling channel	20
Figure 2.7(e)	Temperature distribution for the blade with cooling channel	21
Figure 2.7(f)	Von Misses stress distribution for the blade without cooling channel	22
Figure 2.7(g)	Von Misses stress distribution for the blade with cooling channel	22
Figure 3.1	Flowchart of the Project Procedure/Development	23
Figure 3.2(a)	Actual Rotor Turbine Blade	25

Figure 3.2(b)	Overview of the Turbine Blade Model	27
Figure 3.2(c)	Overview of the imported (from CATIA) Turbine Blade Model in ANSYS FLUENT Design Modeler	30
Figure 3.2(d)	Overview of the meshed model in fluid flow (FLUENT)	31
Figure 3.2(e)	Overview of the model in FLUENT for simulation	31
Figure 3.2(f)	Overview of the imported (from CATIA) Turbine Blade Model in ANSYS	32
Figure 3.2(g)	Overview of the meshed turbine blade model	33
Figure 3.2(h)	Overview of the loads applied on the turbine blade model	35
Figure 3.2(i)	Overview of the Turbine Blade Model with External and Pin fin cooling hole	37
Figure 3.2(j)	Overview of the loads applied on the turbine blade model with external and pin-fin holes	39
Figure 3.2(k)	First Stage Rotor Blade with cooling ducts and film cooling orifices	40
Figure 3.2(l)	Overview of the Turbine Blade Model with 9 cooling channels	41
Figure 4.1(a)	Fluid flow velocity streamline along the turbine blade model surface	43
Figure 4.1(b)	Fluid flow velocity vectors colored by velocity magnitude of the turbine blade	44
Figure 4.2	Temperature distribution for the blade model	45
Figure 4.3	Temperature distribution for the blade model with external and pin-fin holes	49
Figure 4.4	Temperature distribution for the blade model with 9 cooling channels	51

LIST OF TABLES

Table 2.6(a)	Turbine Inlet Stage Operating Conditions	18
Table 2.6(b)	Cooling Channel Inlet Boundary Conditions	18
Table 2.6(c)	Root leading and trailing edge boundary conditions	18
Table 3.2(a)	External Boundary Condition of the blade	29
Table 3.2(b)	Turbine Blade Internal Boundary Conditions	29

CHAPTER 1

INTRODUCTION

1.1 Background of Study

Gas Turbine engine is the engine that converts the energy of the moving stream of fluid into mechanical energy. This gas turbine is an axial flow machine that related to the application of a thermodynamics process known as the simple Brayton cycle.

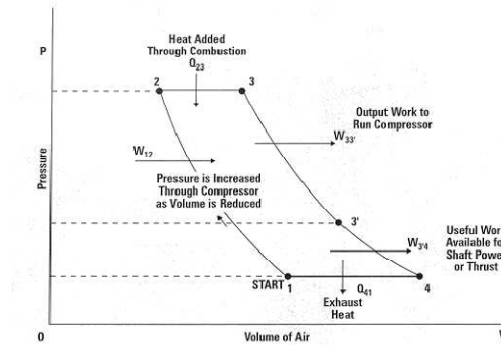


Figure 1.1: Brayton Cycle

The Brayton Cycle (Figure 1.1), as applied to the gas turbine engine, consists of the following four processes which are compression, combustion, expansion and exhaust. The Brayton Cycle taking place in the engine is a smooth continuous process. Firstly, in compression stage, air drawn into the engine and compressed travels into the series of rotating blade. Then, the compress air passes into combustion chamber, gas fuel added, ignite and burn producing hot gas (combustion stage).

In expansion stage, hot gas expands across the turbine rotors driving the shaft that powers turbine air compressor as well as driven equipment, compressor, pump or electrical generator. In this stage, the power turbine blades after the combustion chamber are located at very high pressure and temperature condition. This condition can affect and damage the strength, material and structure of the power turbine blade.

So, an important consideration at the design stage of the gas turbine engine is the need to ensure that certain parts of the engine, and in some instances certain accessories, do not absorb heat to the extent that is detrimental to their safe operation.

Cooling air is used to control the temperature of the gas turbine to ensure an even temperature distribution and therefore improves engine efficiency by controlling thermal growth. One of the methods of the gas turbine cooling air is by continuously cooling the internal of the turbine blade. For this purpose, the project is carried out to investigate the blade surface temperature profile and thermal analysis to ensure proper internal cooling.

1.2 Problem Statement

High thermal efficiency and power output of the gas turbine is dependent upon high turbine entry temperature. The thermal efficiency of the gas turbine can be raised by increasing its maximum operating temperature. Nevertheless, the temperature is limited by the turbine blade materials which cause the failure of the turbine blade structure and strength. One of the methods to prevent this problem is by continuous internal cooling of the turbine blade. The blade of the turbine is air-cooled to achieve low metal temperatures and high blade life integrity and structure. Thus, it is considered important to investigate the blade surface temperature profile and thermal analysis to ensure proper cooling can be performed.

1.3 Objective

The main objectives of this project are:

1. To investigate and analyze the temperature profile along the turbine blade surface.
2. To study on the thermal analysis (fluid flow and heat/temperature distribution) of the turbine blade during the internal cooling process.

1.4 Scope of Study

The scopes of study of the project are:

1. Modeling of the turbine blade
2. Simulation of the model using ANSYS and ANSYS FLUENT
3. Validation using publish data (Literature Review)
4. This project will be excluding the physical experiment
5. Sensitivity study of the model, as examples:
 - Effect of the number and size of holes
 - Effect on the types of holes

CHAPTER 2

LITERATURE REVIEW AND THEORY

2.1 Concept of Turbine Blade Cooling

Gas Turbine engines operate at high temperatures to improve thermal efficiency and power output. As the turbine inlet temperature increases, the heat transferred to the turbine blades also increases. The level and variation in the temperature within the blade material must be limited to achieve reasonable durability goals.

The operating temperatures are far above the permissible metal temperatures. Therefore, there is a need to cool the blades for safe operation. The blades are cooled by extracted air from the compressor of the gas turbine. Since this extraction incurs a penalty to the thermal efficiency, it is necessary to understand and optimize the cooling technique, operating conditions and turbine blade geometry [1].

Gas turbine blades are cooled internally and externally. The external cooling technique includes film cooling and the internal cooling techniques consist of impingement cooling, rib-turbulated cooling and pin-fin cooling. For this project, the author will only cover the internal blade cooling. Internal cooling is achieved by passing the air/coolant through several enhanced passages inside the blades and extracting the heat from the outside of the blades. Figures 2.1(a) and 2.1(b) below show the internally cooled high-pressure turbine rotor blade for GE CF6 engine.

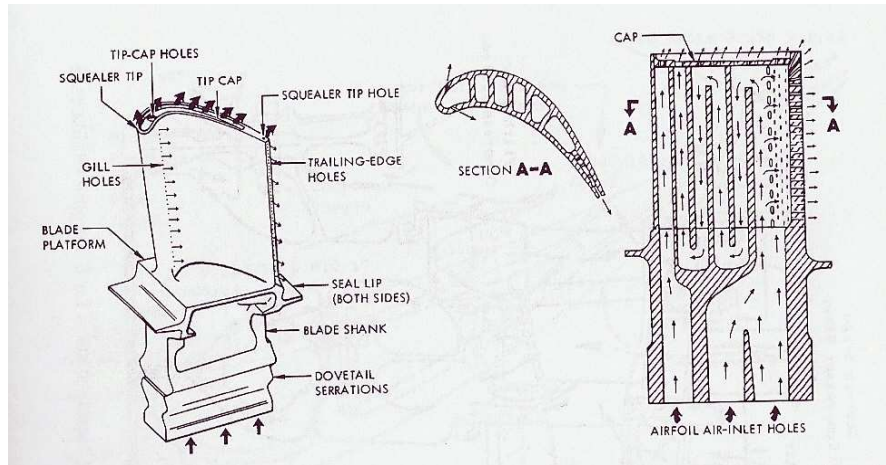


Figure 2.1(a): High pressure turbine rotor blade internally cooled for GE CF6 engine (Treager, 1979)

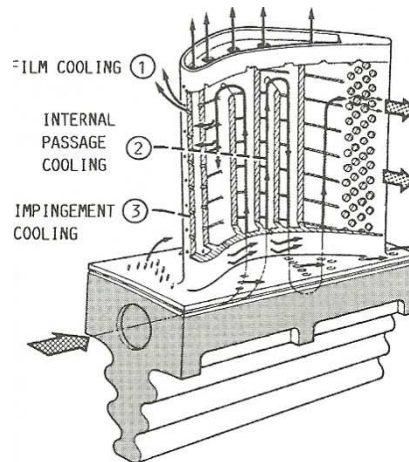


Figure 2.1(b): Typical cooled aircraft gas turbine blade (Gladden and Simoneau, 1988; collected in Sokolowski, 1989)

2.2 Internal Gas Turbine Cooling Systems

Gas turbine-cooling technology is complex and varies from one engine manufacturer to another. However, most of the cooling system designs are quite similar regardless of engine manufacturer and models. Refer to Appendix I and II, the typical turbine cooling system examples are NASA's energy efficient engine (E³), developed by GE Aircraft Engines (Halila et al., 1982) and RB211 24G Rolls Royce Gas Generator. Figure 2.2 draws the cooling concepts of modern, multi-pass turbine rotor blade.

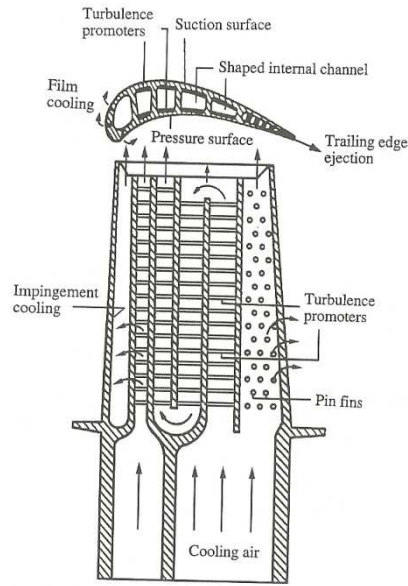


Figure 2.2: Cooling Concepts of a modern multi-pass turbine blade (Han et al., 1984)

From Figure 2.2 above, there are 3 major internal cooling techniques that consist of impingement cooling, rib-turbulated cooling and pin-fin cooling. The blade midchord region uses serpentine coolant air passages with rib turbulators on the inner walls of the rotor blades, while the blade trailing-edge region uses short pins due to space limitation and structure integration. Heat transfer in rotating coolant air passages is very different from that in stationary coolant air passages. Both Coriolis in rotating buoyancy forces can alter the flow and temperature profiles in the rotor coolant air passages and affect their surface-heat-transfer distributions [1].

It is very important to determine the local-heat-transfer distributions in the rotor coolant air passages with impingement cooling, rib-turbulated cooling, or pinned cooling under typical engine cooling flow. Coolant air-to-blade temperature difference (buoyancy effect), and rotating conditions. It is also important to determine the information on the associated coolant air passages pressure losses for a given internal cooling design. This can help in designing an efficient cooling system and prevent local hot-spot overheating of the rotor blade [1].

2.3 Jet-Impingement Cooling

Among all heat-transfer enhancement techniques, impingement has the most significant potential to increase the local heat transfer coefficient. However, the construction of this flow arrangement weakens the structural strength, and therefore this technique is used in the locations where thermal loads are excessively high [1].

In general, there are two locations in turbine blade design where impingement cooled has been used. The first location is used for leading edge cooling as per figure. Dedicated cooling air is allowed to pass through rib cross-over openings leading to impingement on the inner wall of the blade leading edge. After impingement cooling the air flow passes through a series of film holes forming a shower-head arrangement through the turbine leading edge [8].

Internal impingement, convective cooling through the film holes, and film cooling become very effective means to cool this section of the blade with very high heat loads.

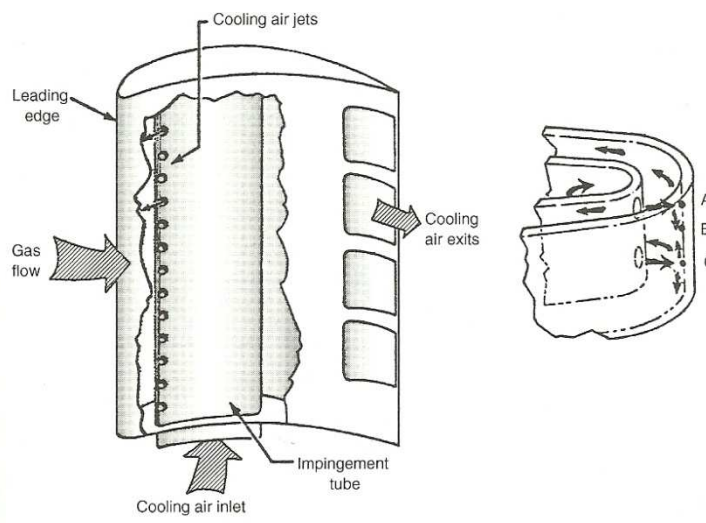


*Figure 2.3(a): Schematic of the impingement cooling at the turbine blades leading edge
(Chupp et., 1968)*

The other location is for trailing edge cooling. In this case, the cooling air is allowed to pass through a series of rib cross-over openings. Jet impingement occurs after each cross-over hole. The air impinges on each subsequent ribs and surrounding walls before discharging at the trailing edge exit slots [9].

The best-equation developed by Chupp et al. (1969) for the impingement heat transfer as follows [1]:

Average Nusselt Number :

$$Nu_{avg} = 0.63 Re^{0.7} \left(\frac{d}{s}\right)^{0.5} \left(\frac{d}{D}\right)^{0.6} \exp \left[-1.27 \left(\frac{l}{d}\right) \left(\frac{d}{s}\right)^{0.5} \left(\frac{d}{D}\right)^{1.2} \right] \quad (1)$$

And the Stagnation Nusselt Number:

$$Nu_{stag} = 0.44 Re^{0.7} \left(\frac{d}{s}\right)^{0.8} \exp \left[-0.85 \left(\frac{l}{d}\right) \left(\frac{d}{s}\right)^1 \left(\frac{d}{D}\right)^{0.4} \right] \quad (2)$$

l = jet to target plate separation distance

d = the jet diameter

s = spacing between jet holes

D = diameter of the target plate

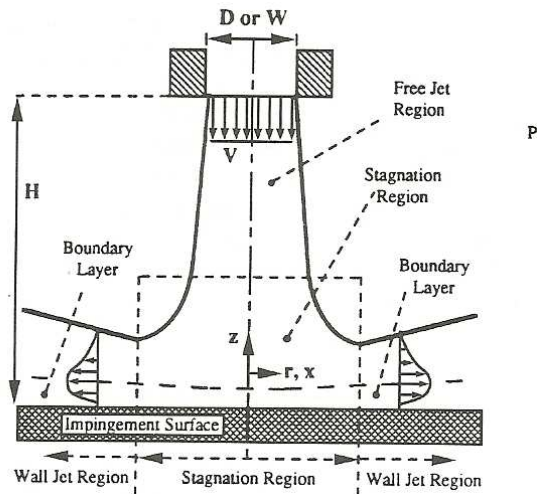


Figure 2.3(b): Flow regions caused by a jet impingement (Viskanta, 1993)

Figure 2.3(b) above shows a typical surface impingement caused by a jet. There exists a stagnation region at the impingement location, and this stagnation region is surrounded by developing boundary layers. Though the convection effects are negligible in the stagnation region (because of zero velocity), the stagnation point is inherently unstable and moves around within a bound. Moreover, a cooling jet has a significantly higher momentum than its surroundings, and the spent jet after impingement creates a highly turbulent flow.

The turbulence intensity at the core can be significantly high. The high velocity coupled with high velocity fluctuation will increase turbulence mixing, increase the heat transfer enhancement capability of the jet significantly. However, there are design constraint and structural integrity problems with jet impingement. To create a jet impingement effect, a surface needs to be perforated, thus weakening the strength of the components [1].

2.4 Rib-Turbulated Cooling

In blade cooling passages, repeated roughness elements in the form of regularly spaced ribs are used to increase and enhance heat transfer rates. Thermal energy conducts from the external pressure and suction surfaces of turbine blades to the inner zone, and the heat is extracted by internal cooling. Han (1984) identified that the heat transfer performance in a stationary ribbed channel primarily depends on the channel aspect ratio, the rib configuration, and the flow Reynolds number. Figure 2.4(a) below shows the specific configurations that characterize a ribbed channel include geometrical features like rib height, pitch and angle of attack [1].

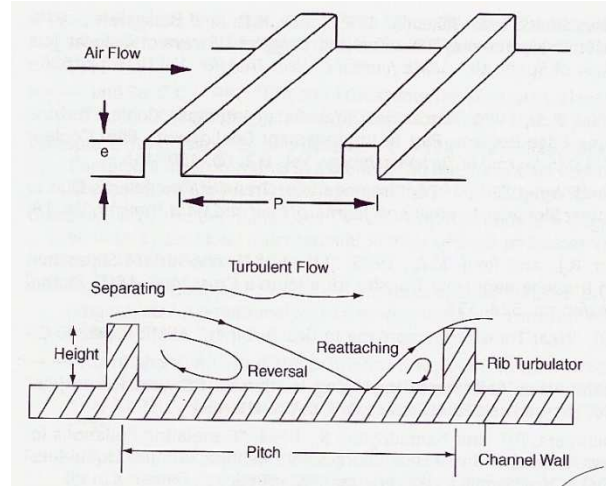


Figure 2.4(a): Schematic Flow separation and rib orientations in heat-transfer coefficient enhancement (Han and Dutta ,1995)

From Figure 2.4(a) above, the ribs in a channel is to increase the rate of heat transfer from the channel walls to the bulk air. This is accomplished by two distinct mechanisms. First, the placement of ribs act as turbulators to break-up the near wall flow increasing the turbulence level and enhancing the exchange of fluid in the near wall region with the core flow by action turbulent diffusion. While this increases the heat transfer, it also increases the wall friction resulting in higher pressure losses. A second heat transfer mechanism is active if the ribs are inclined to the core flow direction. In this case, the ribs induce secondary flows (reversal flow) in the core flow, which can circulate air from the middle of the channel towards the walls thus increasing the heat transfer along these walls. The secondary flows have a smaller effect on the pressure losses, thus they are more beneficial of increasing the thermal performance of the cooling channel [10].

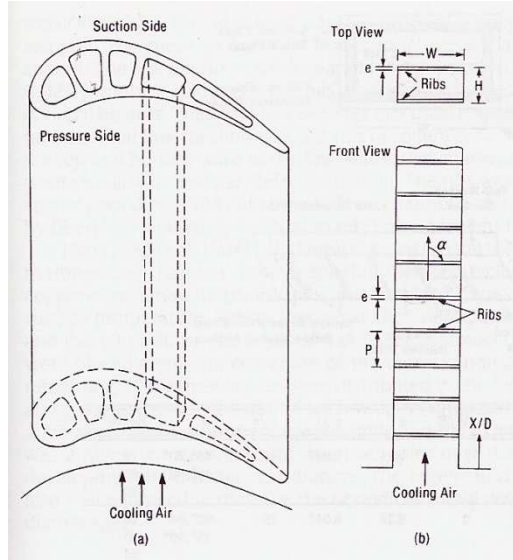


Figure 2.4(b): Typical coolant channels in the turbine blade and internal rib arrangement (Han, 1988)

Figure 2.4(b) above shows the orientation of a typical coolant channel in a turbine blade. Normally, the suction and pressure sides are ribbed. Analytical methods for predicting the friction factor and heat transfer coefficient for turbulent flow over rib-roughened surface are not available because of the complex flow created by periodic rib-roughness elements such as separation, reattachment, and recirculation.

As the theory of the concept from Nikuradse (1950) and Dipprey and Sabersky (1963), the laws of the wall in fully developed turbulent flow can be expressed by the velocity and temperature profiles normal to the rough surfaces as [1]:

$$u^+ = 2.5 \ln \left(\frac{y}{e} \right) + R(e^+) \quad (3)$$

$$T^+ = 2.5 \ln \left(\frac{y}{e} \right) + G(e^+, Pr) \quad (4)$$

u^+ and T^+

= dimensionless velocity and temperature at the distance y from the rough wall

e = height of the ribs

$R(e^+)$ and $G(e^+, Pr)$

= dimensionless velocity and temperature at tip of the ribs, i.e., at $y = e$

Han (1988) developed a correlation to predict the performance of two sided orthogonal ribbed rectangular channel. The roughness R was given by:

$$R(e^+) = \left(\frac{2}{f}\right)^{0.5} + 2.5 \ln \left(\frac{2e}{D} \frac{2W}{W+H}\right) + 2.5 \quad (5)$$

The heat transfer roughness function G was given by:

$$G(e^+, Pr) = R(e^+) + \frac{\left(\frac{f}{2ST_R}\right)^{-1}}{\left(\frac{f}{2}\right)^{0.5}} \quad (6)$$

The roughness Reynolds number e^x is given by:

$$e^x = \left(\frac{e}{D}\right) Re \left(\frac{f}{2}\right)^{0.5} \quad (7)$$

$$\text{Four sided rib channel friction factor, } f = \bar{f} + \left(\frac{H}{W}\right)(\bar{f} - f_s) \quad (8)$$

\bar{f} = friction factor in a channel with two opposite ribbed walls

f_s = friction factor for four smooth sided channel

H = Flow channel height

W = Flow channel width

H = Flow channel height

ST_R = ribbed sidewall average Stanton Number

2.5 Pin-Fin Cooling

In trailing edge designs, typically two rows of cross-over holes are used for cooling. The flow acceleration is high through these cross-over impingement openings. The coolant flow Mach number profiles follows that of the coolant static pressure profile in that it assumes almost stepwise profiles as the cooling flow crosses through these openings. The step-wise profiles are undesirable as they lead to relative high peaks in internal heat transfer coefficients at the walls of the blade.

In other words, there are regions in the blade trailing edge walls, which attain relative lower metal temperatures due to high internal heat transfer coefficients. Meanwhile, other areas attain relatively higher metal temperatures due to lower internal heat transfer coefficients. These metal temperature differences can lead to high thermal strains, which in conjunction with transient thermal response during power loading can, in turn, lead to undesirable thermal-mechanical fatigue damage [10].

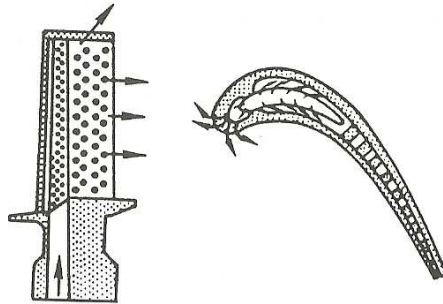


Figure 2.5(a): The trailing edge of the turbine blade is cooled by pin fins (Metzger et al., 1984)

It is, therefore, desirable to use a trailing edge cooling design as per Figure 2.5(a), which improves the internal profiles for Mach number, static pressure drop, and internal heat transfer coefficient distributions along the blade trailing edge. In that regard, internal features, such as pedestals provide design advantages. As examples, Figure 2.5(b) shows the four typical ejection hole configurations used by Lau et al. (1989a). Optimum designs may include internal pedestals with many different cross-sectional areas, such as: circular, oval, racetrack, square, rectangular, diamond cross-sections, and others. Mostly, attention is given to the simplest form of an internal cooling feature: such as round pedestals [10].

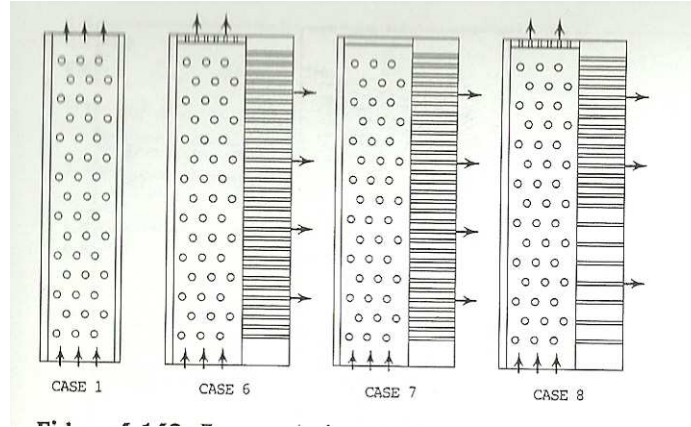


Figure 2.5(b): Four typical ejection hole configurations used by Lau et al. (1989a)

The relevant cooling characteristics of round pedestals could easily be extended to other cross-sectional area pedestals for specific applications. In this context, for a staggered array of round pedestals the internal unobstructed trailing edge channel area will have a cross-sectional area [10]:

$$A = WH \quad (9)$$

W = width of the channel

H = height of the channel

The corresponding perimeter becomes;

$$Per = 2(W + H) \quad (10)$$

And the hydraulic diameter is given by;

$$dH = \frac{4A}{Per} \quad (11)$$

The surface area becomes

$$A_{duct} = 2WL \quad (12)$$

L = length of the channel

The surface of the plate not being covered by the pedestals becomes:

$$A_{plate} = A_{duct} - 2(N_L N_T) [\pi (\frac{d_{pin}^2}{4})] 2WL \quad (13)$$

N_L and N_T = number of pedestals in the longitudinal and transverse directions of the trailing edge channel

It should be noted that the number of pedestals can be given by:

$$N_T = \frac{W}{S_n} \quad (14)$$

$$N_L = \frac{L}{S_p} \quad (15)$$

S_n and S_p = transverse and longitudinal pitches

With these geometrical parameters, the Reynolds number, associated with the pin diameter, is calculated as follows:

$$Re_d = \rho d_{pin} V_{max} / \mu \quad (16)$$

$$V_{max} = V \left(\frac{A}{A_{min}} \right) \quad (17)$$

$$A_{min} = (W - N_T d_{pin}) H \quad (18)$$

V = free stream inlet velocity

2.6 Design Geometry and Boundary Condition

Usually, the analysis begins with the modeling of a 3D section of the blade as a solid model and then proceeds by using a finite element code, such as ANSYS, for completing the thermal-stress analysis. As example, the blade solid model and the corresponding finite element ANSYS model are shown in Figure 2.6(a). As can be seen from the transparent of the solid model, this blade is cooled by convection with cavity wall trip strips and with a set of pedestals in the trailing edge. While external surfaces are locally film cooled from the leading edge with three rows of showerhead holes, there are no film cooling holes on either the pressure or suction surfaces of the airfoil. The trailing edge has a centerline cooling flow ejection [10].

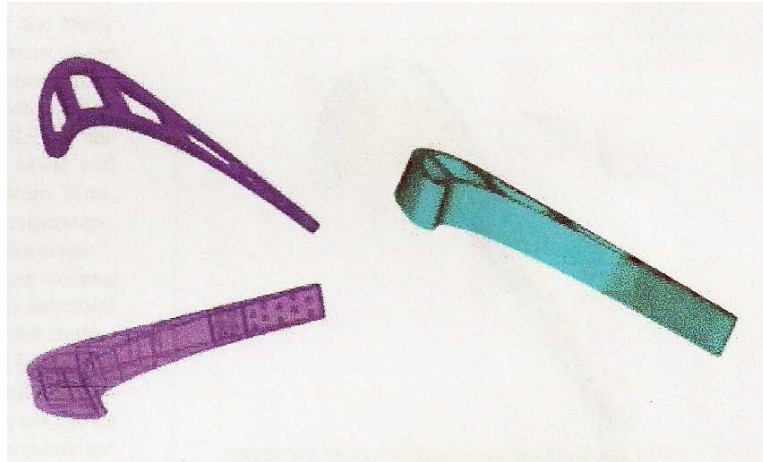


Figure 2.6(a): NASA E³ blade solid model and corresponding finite element ANSYS model

The design of the turbine blade model is based on the research data from [11]. Figure 2.6(b) below shows details of the turbine rotor blade geometric data from the A. Yangyozov and R. Willinger research journal [11]:

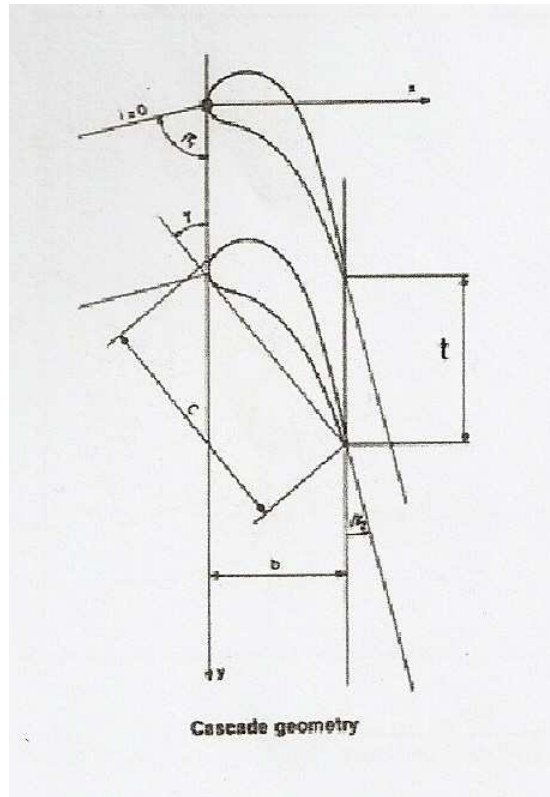


Figure 2.6(b): Turbine blade design geometry

Height, $h = 200$ mm

Pitch, $t = 73$ mm

Chord Length, $c = 100$ mm

Axial Chord Length, $b = 61.85$ mm

Aspect Ratio, $AR = h/c = 1.5$

Inlet Blade Angle (tangential), $\beta_1 = 76.1^\circ$

Outlet Blade Angle (tangential), $\beta_2 = 14.5^\circ$

Stagger Angle, $\gamma = 39.9^\circ$

The operating conditions are given in Table 2.6(a) [12]:

Table 2.6 (a): Turbine Inlet Stage Operating Conditions

Inlet Total Pressure	7×10^5 Pa
Inlet Total Temperature	1350 K
Inlet Mach Number	0.3
Outlet Static Pressure	3.5×10^5 Pa
Outlet Mach Number	0.8
Mass Flow Rate	400 kg/s
Convection Coefficient, h	$3000 \text{ W/m}^2 \text{ K}$

The blade has five cylindrical cooling channels in order to control the temperature and maintain the mechanical integrity. The cooling channel inlet boundary conditions are given in Table 2.6(b) [12].

Table 2.6(b): Cooling Channel Inlet Boundary Conditions

Cooling Channels	1-2	3-5
Total Pressure (Pa)	8×10^5	5×10^5
Total Temperature (K)	600	600

The computational model further assumes no leakage flow through the hub surface. The heat transfer from one blade root to the neighboring one is minimal since they are in contact on both sides and the lateral root surfaces are considered adiabatic. A convective boundary condition is applied to the leading and trailing edge root surfaces. The convective boundary conditions are given in Table 2.6(c) [12].

Table 2.6(c): Root leading and trailing edge boundary conditions

	Root Leading Edge	Root Trailing Edge
Convection Coefficient, h	1000 W/m^2	1000 W/m^2
Fluid Temperature, T_{fluid}	700 K	600 K

2.7 Analysis and Expected Results

For the analysis, the thermal results are shown in Figure 2.7(a), which illustrates a region on the suction side with high metal temperatures corresponding to high thermal loads due to flow acceleration.

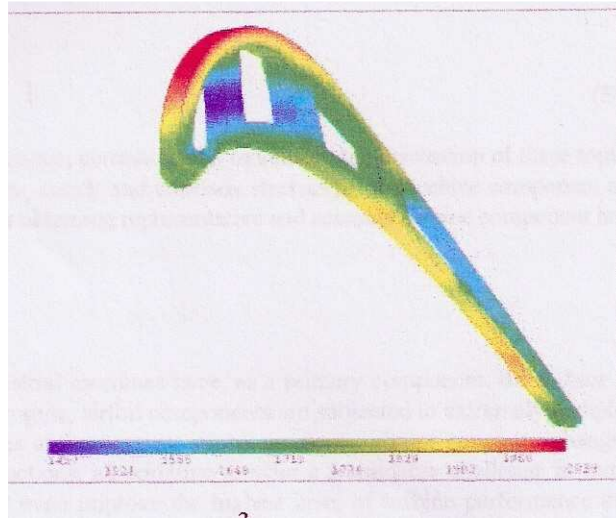


Figure 2.7(a): NASA E³ blade solid thermal results

Furthermore, there is one analysis research on the flow characteristics in heat turbo machinery turbine stage by using ANSYS CFX Software. The main purpose is to investigate the flow characteristics of the rotor turbine blade. The results of the analysis as follow [11]:

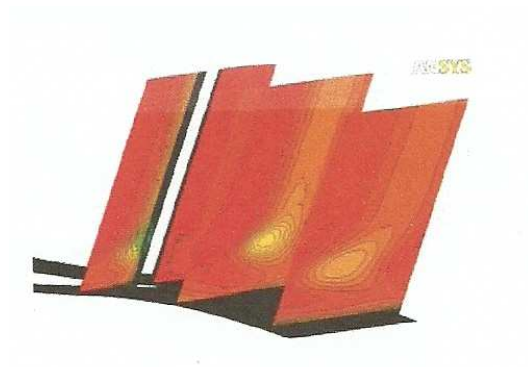


Figure 2.7(b): Total Pressure Contour Lines (Yellow color is vortex core, only lower half blade part is shown)

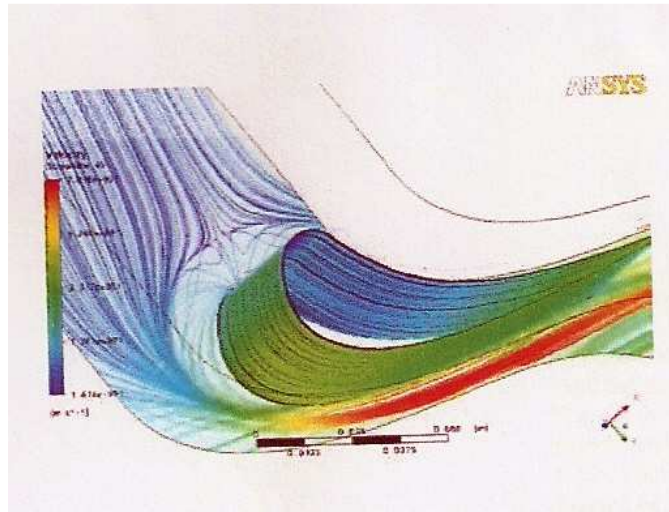


Figure 2.7(c): Streamlines Surface and 3D secondary flow at hub

The impact of the cooling channels is assessed by comparing the results of a blade without cooling with the ones of a blade where the cooling channels are evenly distributed along the camber line. The temperature distribution on the blade surface without cooling channels is shown in Figure 2.7(d).

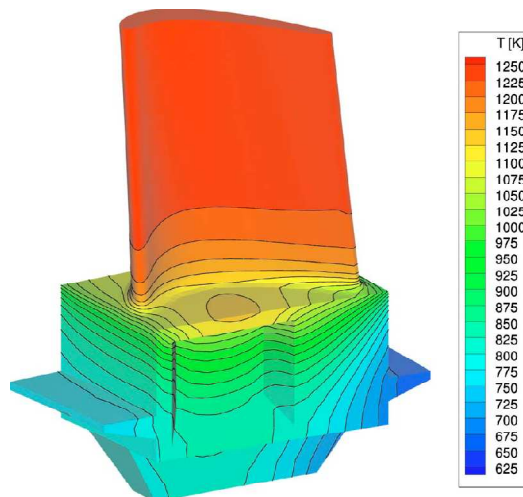


Figure 2.7(d): Temperature distribution for the blade without cooling channel

The maximum material temperature is observed at the trailing edge tip and equals 1249K. A large part of the blade has a temperature above 1200 K. The part of the blade in the main flow field acts as a cooling fin with radially increasing temperature away from the cooling source.

Figure 2.7(e) shows the temperature distribution for the blade with cooling channels. An important reduction in temperature is observed. The major part of the blade cooling is now performed by the cooling channels and the flow in the root cavities has only a small impact on the cooling. The maximum material temperature, again observed at the trailing edge tip, is reduced to 1222 K and only a small part of the blade has a temperature above 1200 K [12].

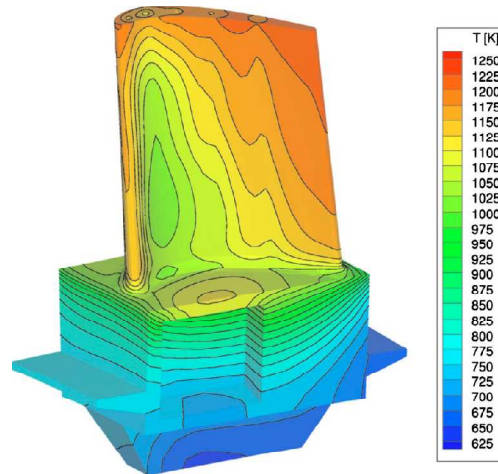


Figure 2.7(e): Temperature distribution for the blade with cooling channel

Thermal stresses for the blade without cooling channels are shown in Figure 2.7(f). As could be expected, the highest values are observed at the junction between blade and hub, where the highest temperature gradients occur. The maximum is located at the hub trailing edge and equals 263 MPa.

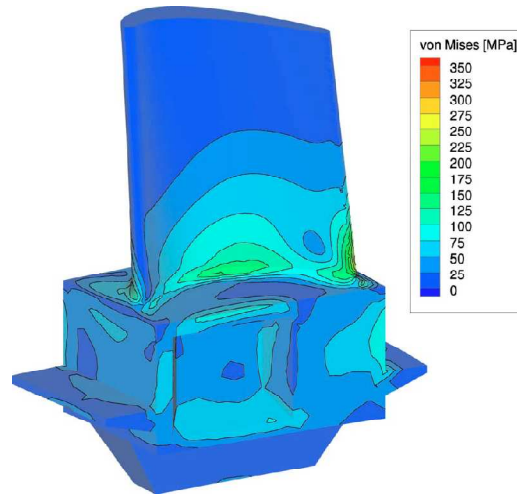


Figure 2.7(f): Von Misses stress distribution for the blade without cooling channel

The thermal stresses for the blade with cooling channels are shown in Figure 2.7(g). They have increased and the maximum value (369 MPa) now appears at the hub leading edge. The variation in the stresses, observed between the midspan and the blade tip, are due to the large temperature gradients induced by the cooling channels. The position of the latter can be recognized by the chordwise variation in the thermal stresses [12].

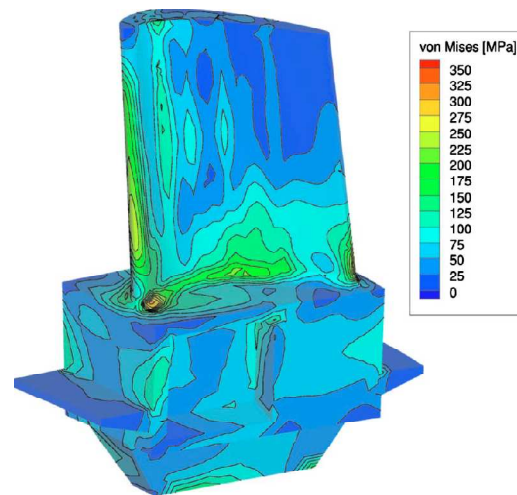


Figure 2.7(g): Von Misses stress distribution for the blade with cooling channel

CHAPTER 3

METHODOLOGY

3.1 Flowchart/Procedure of Project Development

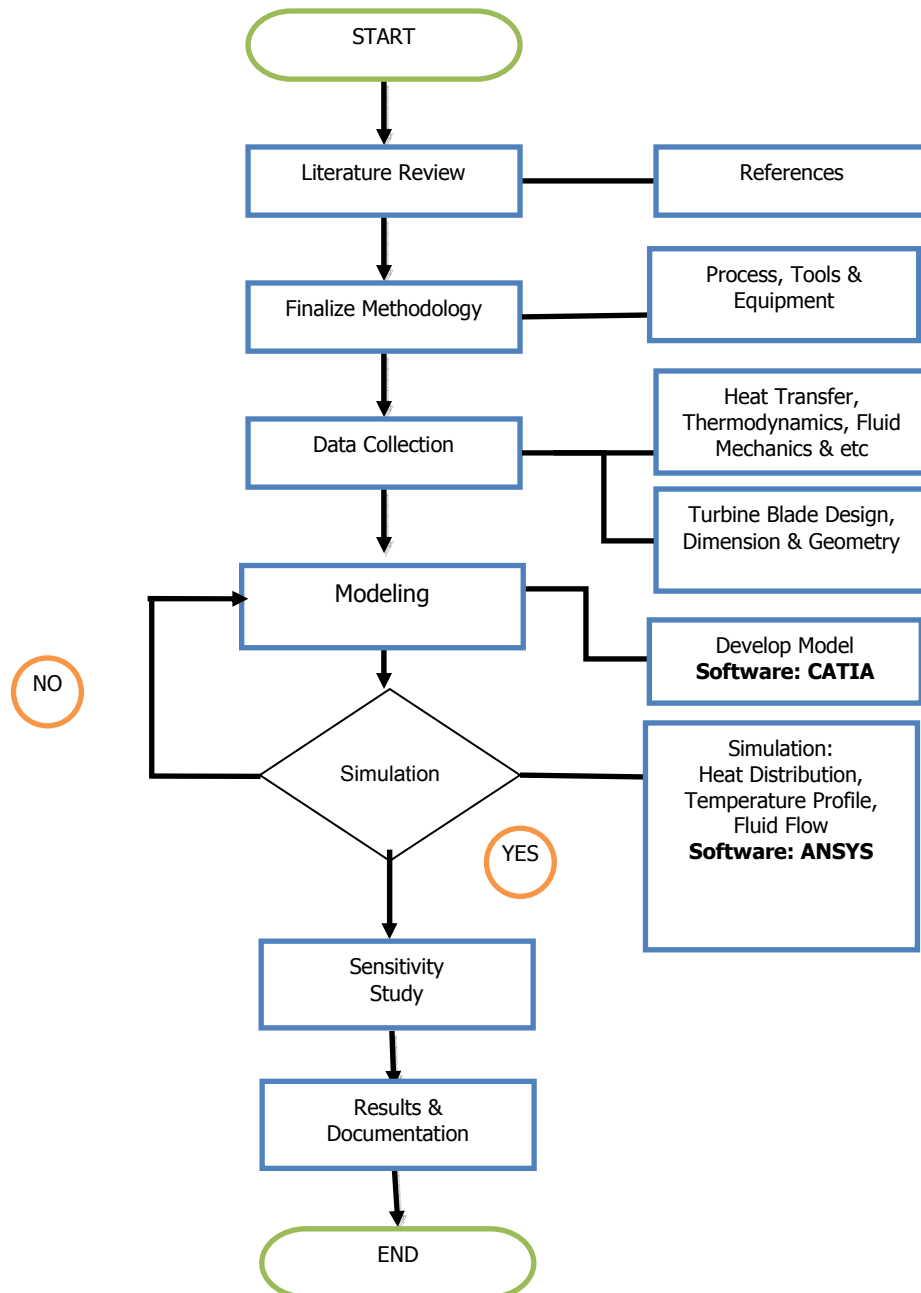


Figure 3.1: Flowchart of the Project Procedure/Development

3.2 Overview of the Methodology

As per the flow chart above, in order to achieve the objectives of the project, research, study and analysis will be done on the gas turbine internal blade cooling system. The following steps and process need to be done:

1. Literature review and data collection on the turbine blade cooling study and analysis

- Literature Review on the researches and the information from the published data as the references for the project
- Includes all the information about the parameter of the data for the analysis, equation and calculations involved, data gathering for the turbine blade design and others.

2. Finalized the procedures, tools and equipment to be used

- The important procedures involved for the project will be modeling and the simulation stage
- As the data collections for the turbine design and thermal analysis will be completed, those stages will be begun and preceded with the result analysis.

3. Modeling and developing the design of the turbine blade

- In the modeling stage, CATIA software will be used based on the design geometry of the turbine blade from the data collection. The details of the modeling stage as follows:

Turbine Blade Design Geometry Data

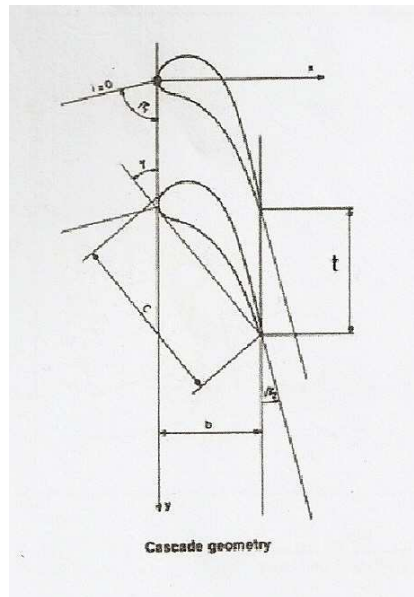


Figure 3.2(a): Actual Rotor Turbine Blade

Pictures above show the actual rotor turbine blade taken from the UTP laboratory. The design and geometry of the model will be based on the actual blade design and from research data from A. Yangyozov and R. Willinger journal [11]. The design blade model is only consists of jet-impingement internal cooling technique with 5 cooling channels.

Development of the Turbine Blade Model using CATIA

At the design stage, the turbine blade model is designed by using the CATIA software. Firstly, the model is designed based on the geometrical data from research data from A. Yangyozov and R. Willinger journal. Details of the design data as follows:



Height, $h = 200 \text{ mm}$

Pitch, $t = 73 \text{ mm}$

Chord Length, $c = 100 \text{ mm}$

Axial Chord Length, $b = 61.85 \text{ mm}$

Aspect Ratio, $AR = h/c = 1.5$

Inlet Blade Angle (tangential), $\beta_1 = 76.1^\circ$

Outlet Blade Angle (tangential), $\beta_2 = 14.5^\circ$

Stagger Angle, $\gamma = 39.9^\circ$

After that, the design will be extruded and padded to get the three dimensional model. Figure 3.2(b) below shows the three dimensional model of the blade with five channels of the internal cooling passages.

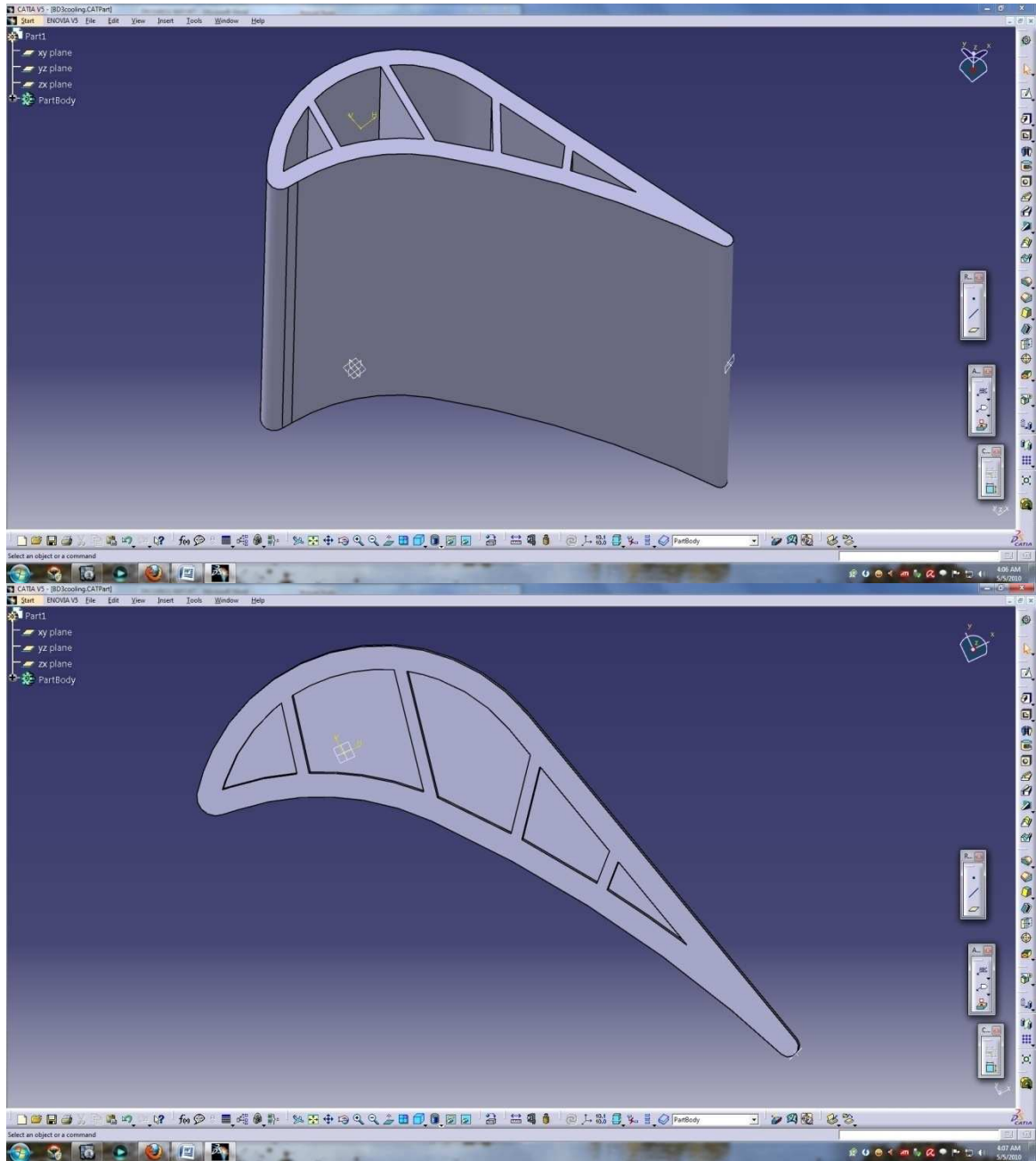


Figure 3.2(b): Overview of the Turbine Blade Model

4. Simulation of the designed turbine blade model

- In simulation stage, the analysis will be divided into two types of the thermal analysis.
- For the fluid flow (velocity vectors and velocity streamlines) analysis, ANSYS FLUENT software will be used.
- For the heat distribution and heat thermal stress, ANSYS software will be used. The details of the simulation stage as follows:

Turbine Blade Boundary Conditions

The results of the analysis will be based on the boundary conditions parameter of the operating condition gas turbines. The boundary conditions of the analysis consist of:

I. Fluid and Solid Material Behaviors

Fluid Material:

- Air
- Density of air = ideal gas
- Specific Heat Capacity, $C_p = 1006.43 \text{ J/kg}\cdot\text{K}$ (constant)
- Molecular Weight = 28.966 mol^{-1}

Solid Material:

Titanium Alloys

Structural	
Young's Modulus	9.6e+010 Pa
Poisson's Ratio	0.36
Density	4620. kg/m ³
Thermal Expansion	9.4e-006 1/°C
Tensile Yield Strength	9.3e+008 Pa
Compressive Yield Strength	9.3e+008 Pa
Tensile Ultimate Strength	1.07e+009 Pa
Thermal	
Thermal Conductivity	21.9 W/m·°C
Specific Heat	522. J/kg·°C
Melting Point	1550-1750 K
Electromagnetic	
Relative Permeability	10000
Resistivity	1.7e-006 Ohm·m

II. Properties of the Boundaries

The operating conditions of the turbine are given in Table 3.2(a). The operating conditions of the turbine inlet stage show the external boundary layer condition of the wall temperature:

Table 3.2(a): External Boundary Condition of the blade

Inlet Total Pressure	7×10^5 Pa
Inlet Total Temperature	1350 K
Inlet Mach Number	0.3
Mass Flow Rate	400 kg/s
Convection Coefficient, h	$3000 \text{ W/m}^2 \text{ K}$

Table 3.2(b) below shows the internal boundary condition of the cooling turbine blade that consists of total pressure, coolant air temperature and internal heat convection coefficient.

Table 3.2(b): Turbine Blade Internal Boundary Conditions

Cooling Channels	1-2	3-5
Total Pressure (Pa)	8×10^5	5×10^5
Coolant Air Temperature (K)	600	600
Internal Convection Coefficient, h ($\text{W/m}^2 \text{ K}$)	1000	1000

Simulation of Turbine Blade Model using ANSYS FLUENT

After the design stage, the simulation stage starts using Fluid Flow analysis software (FLUENT) for completing the velocity streamline and velocity vectors analysis along the turbine blade. The model from CATIA is imported to the ANSYS FLUENT to begin the analysis and the analysis being made in the FLUENT software as per Figures 3.2(c), 3.2 (d) and 3.2(e) below.

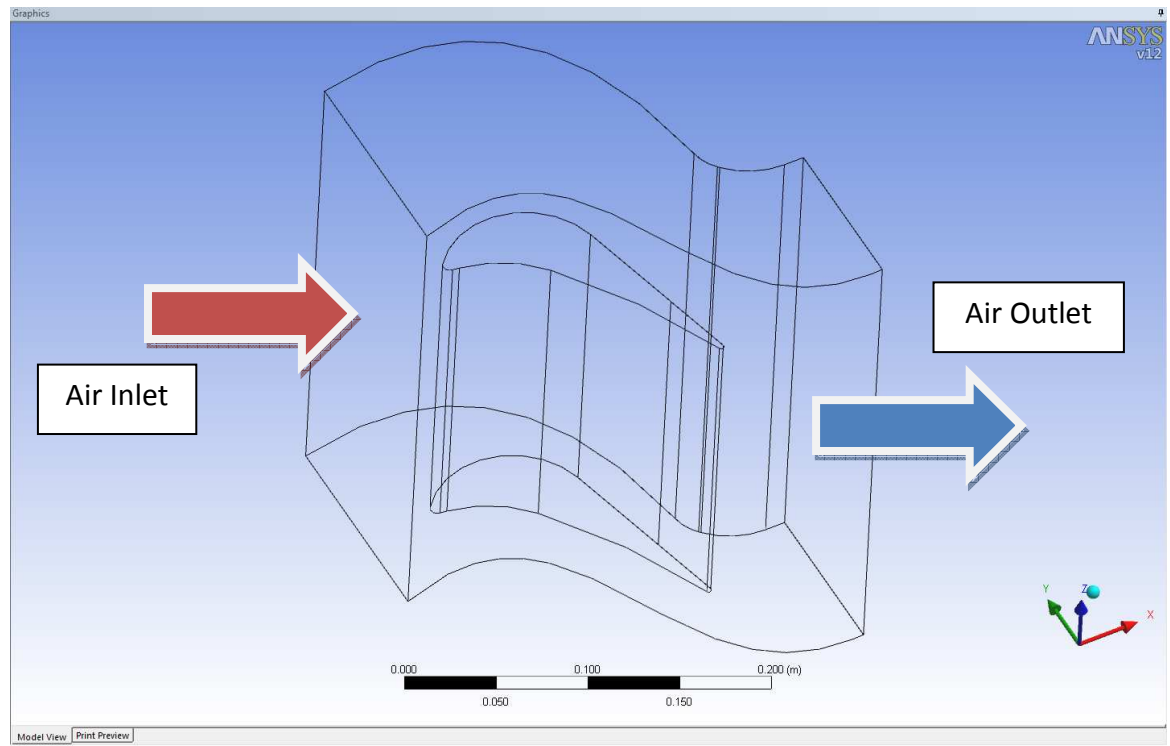


Figure 3.2(c): Overview of the imported (from CATIA) Turbine Blade Model in ANSYS FLUENT Design Modeler

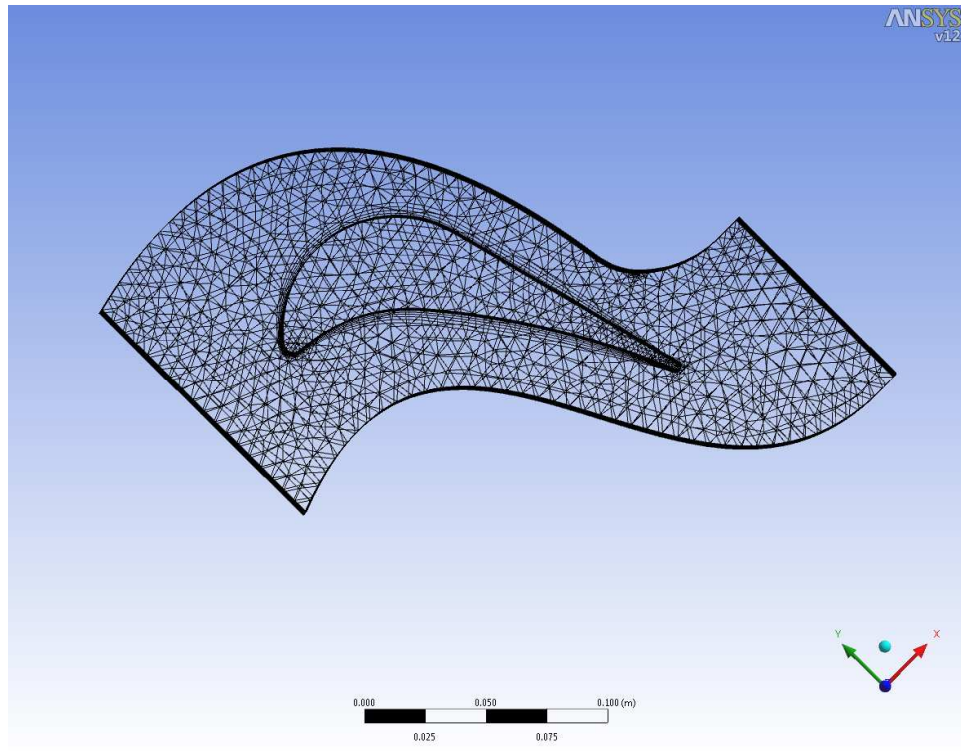


Figure 3.2(d): Overview of the meshed model in fluid flow (FLUENT)

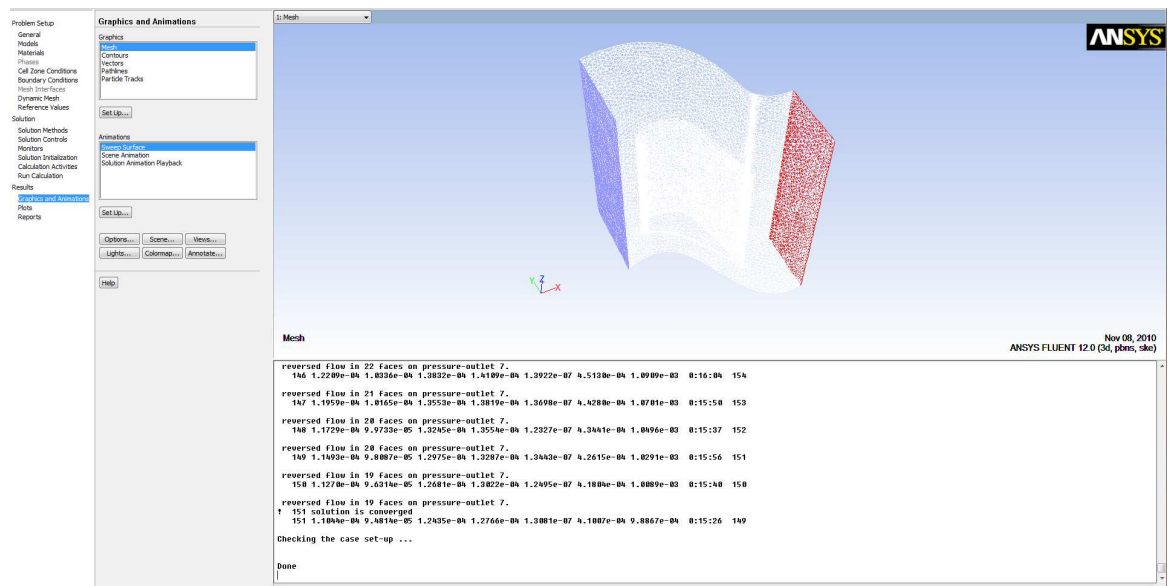


Figure 3.2(e): Overview of the model in FLUENT for simulation

Simulation of Turbine Blade Model using ANSYS

After the design stage, the simulation stage starts using finite element software (ANSYS) for completing the thermal-stress analysis to analyze the heat distribution along the turbine blade. The model from CATIA is imported to the ANSYS to begin the analysis stage as per Figure 3.2(f).

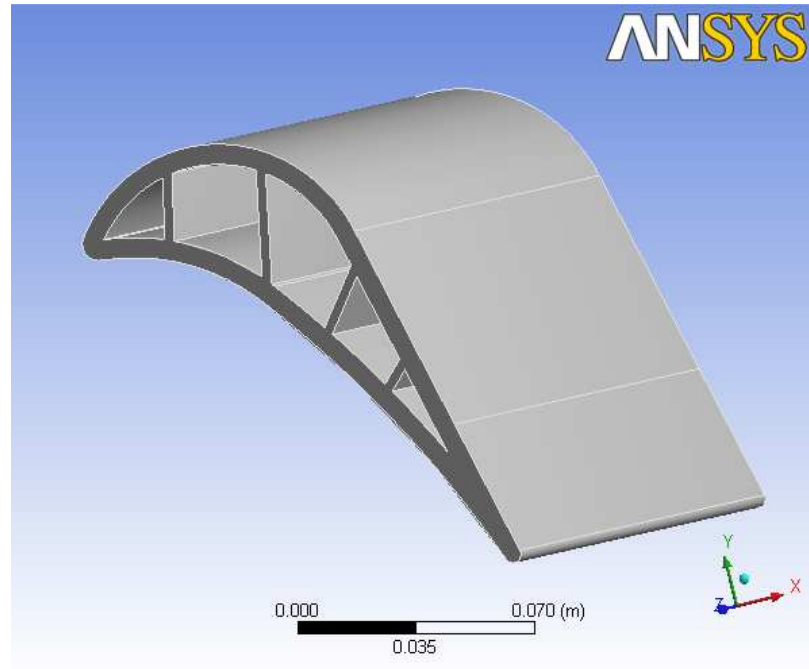


Figure 3.2(f): Overview of the imported (from CATIA) Turbine Blade Model in ANSYS

- Mesh

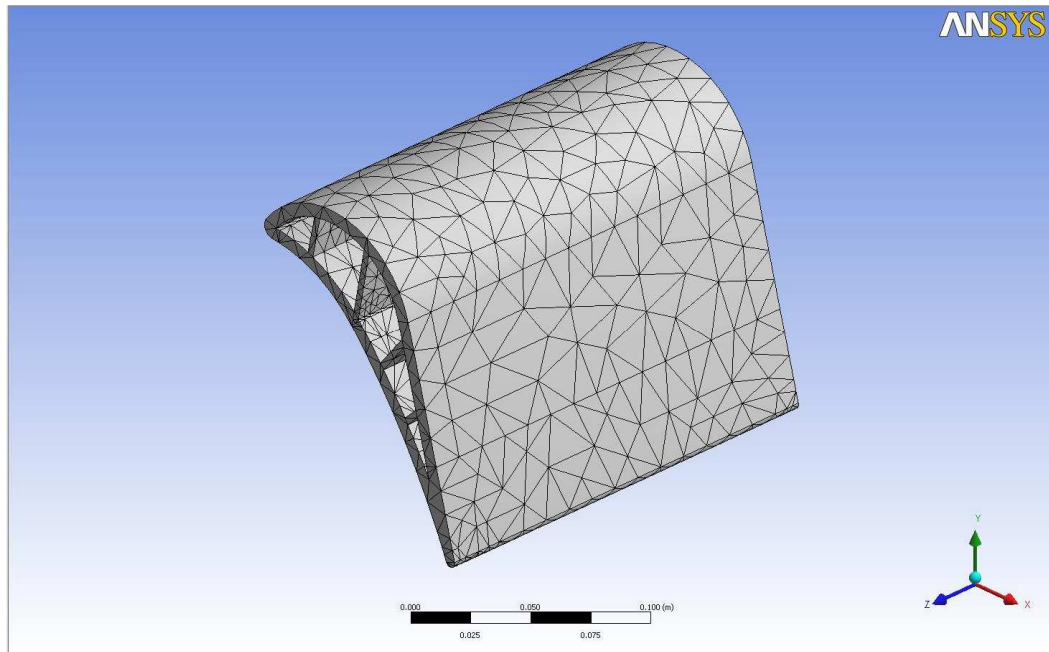


Figure 3.2(g): Overview of the meshed turbine blade model

Summary of Turbine Blade Geometry

Object Name	<i>Turbine Blade</i>
State	Meshed
Definition	
Material	Titanium Alloy
Stiffness Behavior	Flexible
Bounding Box	
Length X	0.1119 m
Length Y	0.14242 m
Length Z	0.201 m
Properties	
Volume	4.8666e-004 m ³
Mass	2.2484 kg
Statistics	
Nodes	10520
Elements	5408

- **Steady-state Thermal Analysis**

A steady-state thermal analysis calculates the effects of steady thermal loads on the blade model. This steady-state thermal analysis is applied to determine temperatures/heat distribution in the model that is caused by thermal loads that do not vary over time. This steady-state thermal analysis is linear, with constant material properties. The details of the model steady-state thermal analysis stage as follows:

Initial Condition of Analysis

Object Name	<i>Initial Condition</i>
State	Fully Defined
Definition	
Initial Temperature	Uniform Temperature
Initial Temperature Value	1077. °C

Loads Apply on the Turbine blade Model

Object Name	Convection	Convection 2	Convection 3	Convection 4
State	Fully Defined			
Scope				
Scoping Method	Geometry Selection			
Geometry	4 Faces	2 Faces		28 Faces
Definition				
ID	28	29	30	39
Type	Convection			
Film Coefficient	3000. W/m².°C (ramped)	3000. W/m².°C (ramped)	3000. W/m².°C (ramped)	1000. W/m².°C (ramped)
Ambient Temperature	1077. °C (ramped)	1077. °C (ramped)	1077. °C (ramped)	327. °C (ramped)

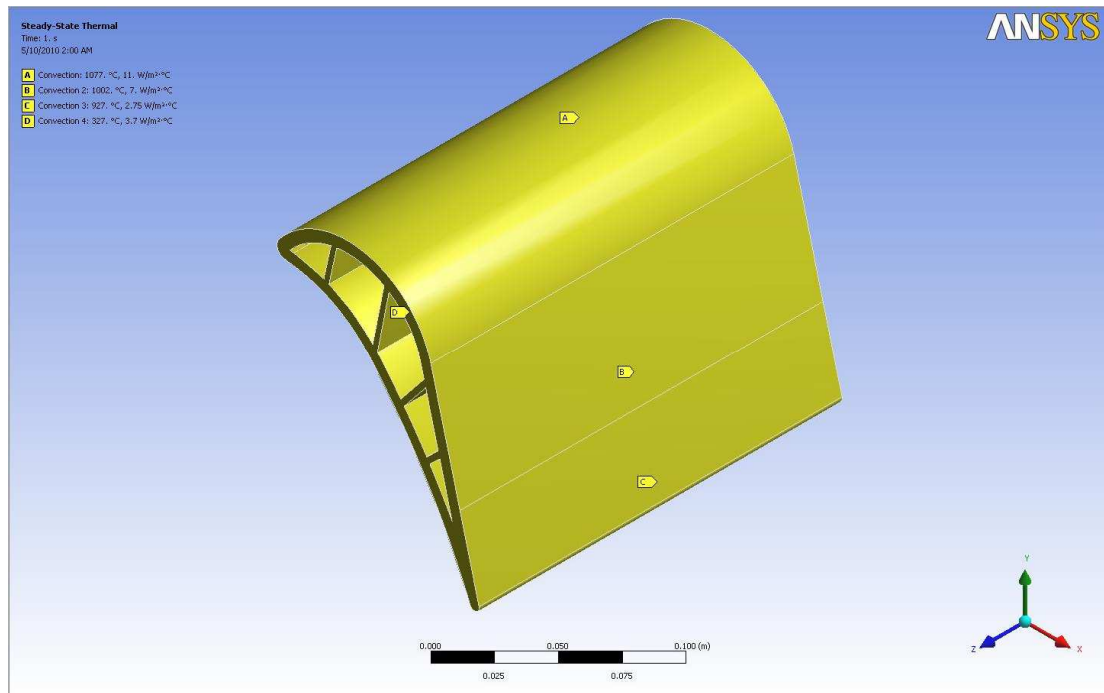


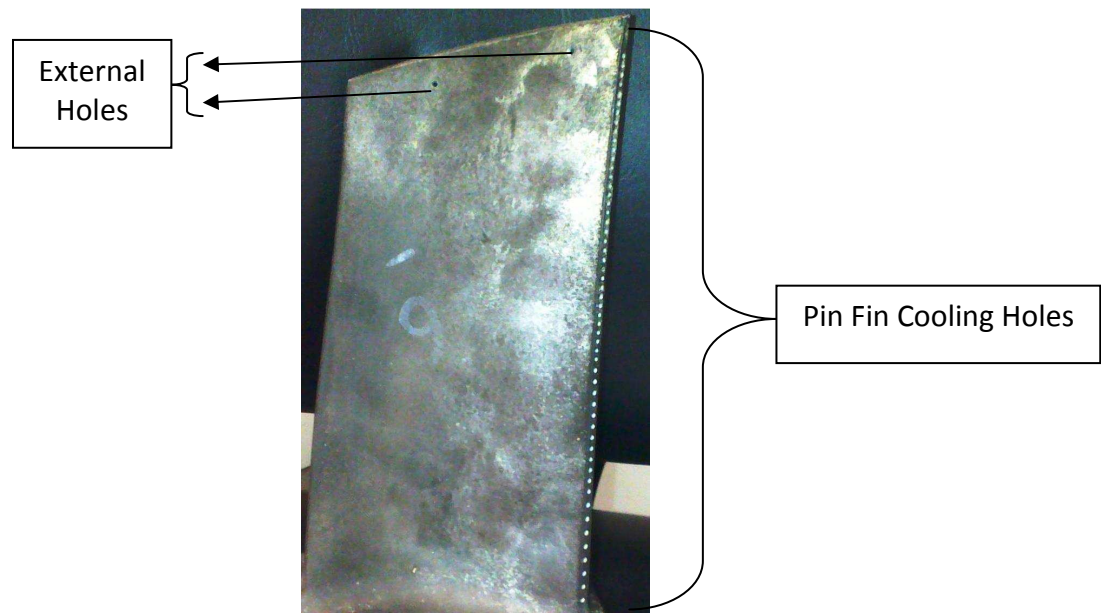
Figure 3.2(h): Overview of the loads applied on the turbine blade model

5. Sensitivity Study on the Turbine Blade Model

- The objective of this sensitivity study is to observe for the change in the result of the thermal analysis of the turbine blade when one of the parameter designs change. As examples, the effect of the number, sizes and types of holes at the turbine blade.
- At this stage, firstly the development of the turbine blade model takes place. Then, the model will be simulated and analyzed by using the same operating boundary condition.
- The design and parameter of the previous base model will be changed to observe the difference on the heat distribution on the turbine blade.

Development of the Turbine Blade Model with External and Pin-Fin Holes

At this sensitivity study stage, firstly, the author will look on the effect of the external holes and pin fin holes at the trailing edge. The actual internal design of the turbine blade is difficult to get because of the gas turbine manufacturer's policy. So, the internal design and geometry of the model will be based on the assumption of scale actual blade design with 5 cooling channels [11]. Details of the design data as follows:



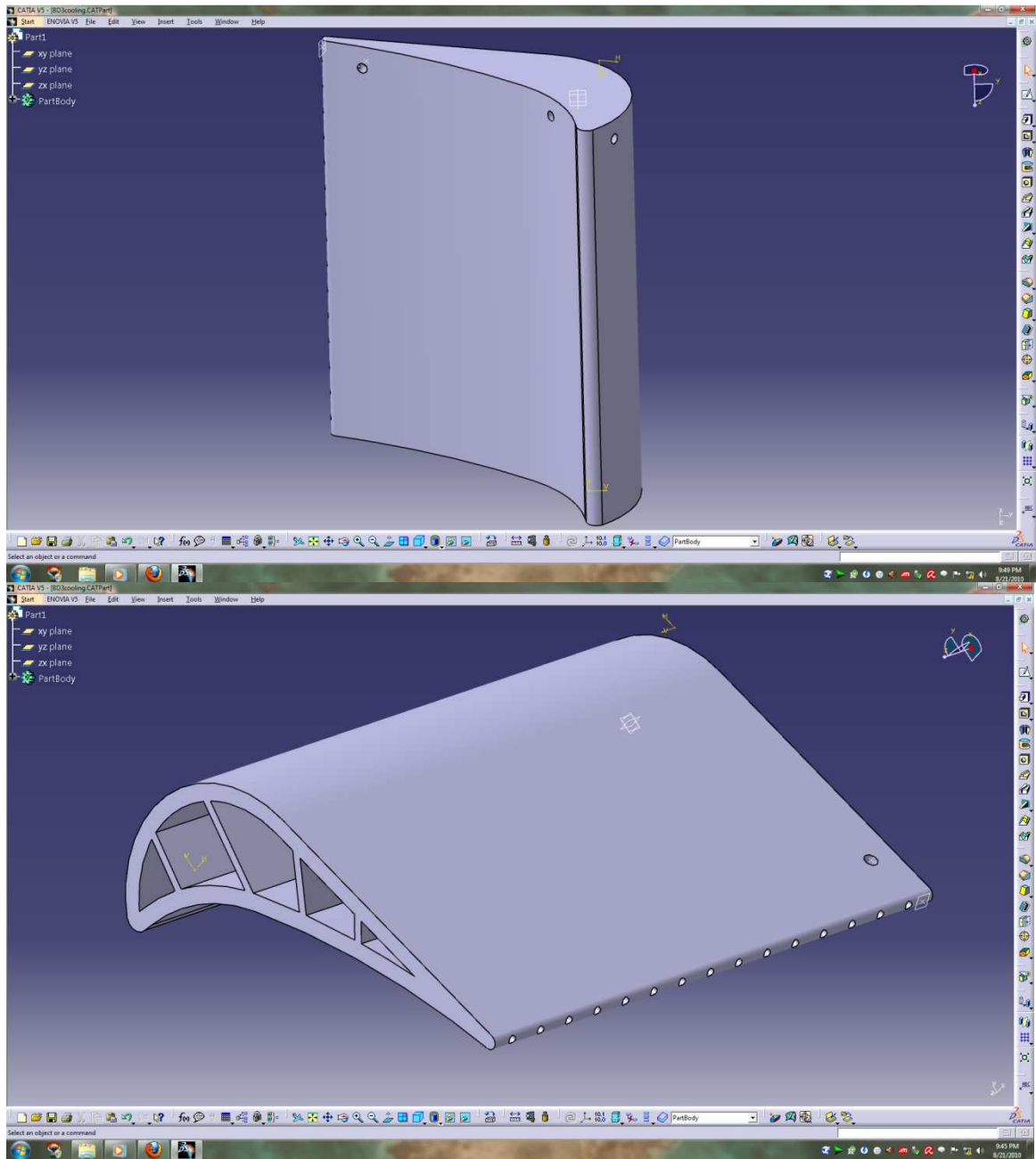


Figure 3.2(i): Overview of the Turbine Blade Model with External and Pin fin cooling hole

Simulation of Turbine Blade Model

This simulation of the new turbine blade model with external and pin-fin holes will be based on the previous boundary conditions parameter of the operating condition gas turbines as above. The model will be divided into two steps that is meshing and steady state thermal analysis. The details of the simulation stage as follows:

Summary of Turbine Blade Geometry

Object Name	<i>Hole Turbine Blade</i>
State	Meshed
Definition	
Material	Titanium Alloy
Stiffness Behavior	Flexible
Bounding Box	
Length X	0.11189 m
Length Y	0.14233 m
Length Z	0.201 m
Properties	
Volume	4.8049e-004 m ³
Mass	2.2199 kg
Statistics	
Nodes	20984
Elements	10894

Initial Condition of Analysis

Object Name	<i>Initial Condition</i>
State	Fully Defined
Definition	
Initial Temperature	Uniform Temperature
Initial Temperature Value	1077. °C

Loads Apply on the Turbine blade Model

Object Name	Convection	Convection 2	Convection 3	Convection 4	Convection 5
State	Fully Defined				
Scope					
Scoping Method	Geometry Selection				
Geometry	4 Faces	2 Faces		28 Faces	6 Faces
Definition					
ID	23	24	25	26	53
Type	Convection				
Film Coefficient	3000. W/m ² .°C (ramped)	3000. W/m ² .°C (ramped)	3000. W/m ² .°C (ramped)	1000. W/m ² .°C (ramped)	
Ambient Temperature	1077. °C (ramped)	1077. °C (ramped)	1077. °C (ramped)	327. °C (ramped)	

Object Name	<i>Convection 6</i>
State	Fully Defined
Scope	
Scoping Method	Geometry Selection
Geometry	30 Faces
Definition	
ID	58
Type	Convection
Film Coefficient	1000. W/m ² ·°C (ramped)
Ambient Temperature	327. °C (ramped)

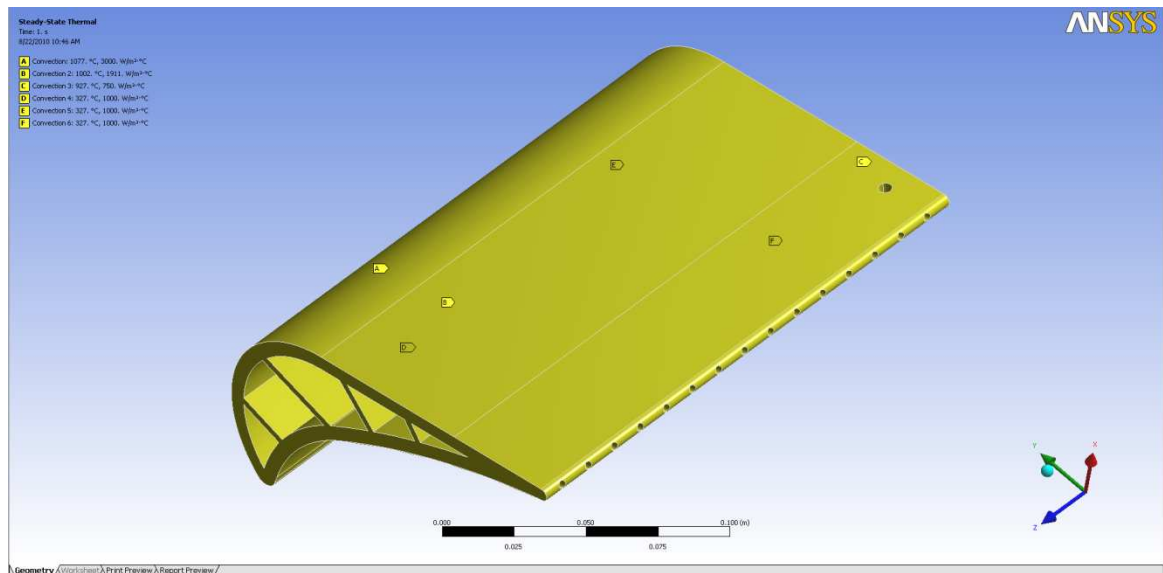


Figure 3.2(j): Overview of the loads applied on the turbine blade model with external and pin-fin holes

Development of the Turbine Blade Model with 9 Cooling Channels

After that, the author looks on the effect of different number of cooling channel with 9 passages. For this design, the model is taken based on the research by the journal as Figure 3.2(k) below [13]. The details of the design as below:

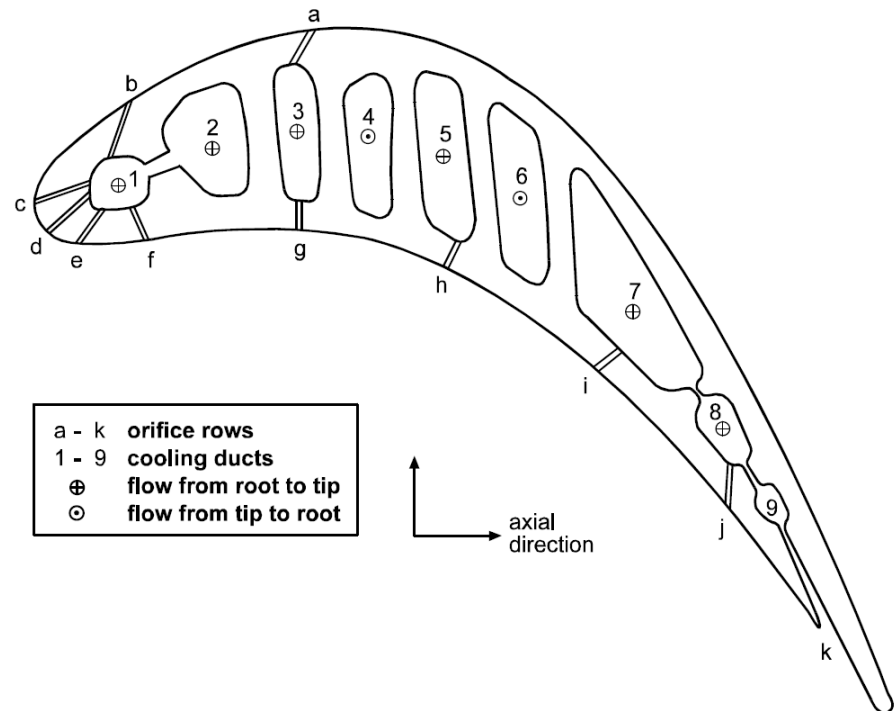


Figure 3.2(k): First Stage Rotor Blade with cooling ducts and film cooling orifices

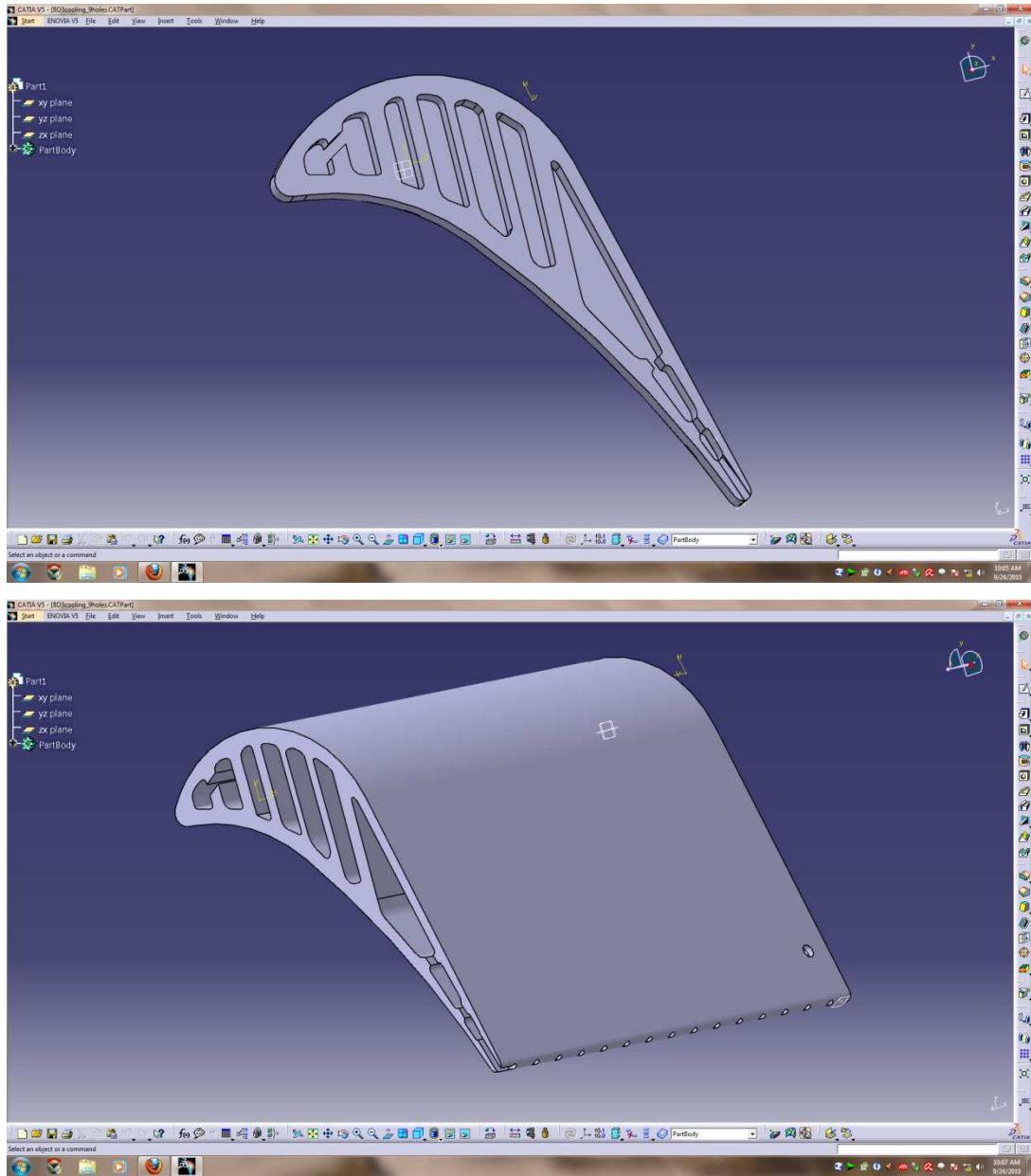


Figure 3.2(l): Overview of the Turbine Blade Model with 9 cooling channels

Simulation of Turbine Blade Model

This simulation of the new turbine blade model with 9 cooling channels will be based on the previous boundary conditions parameter of the operating condition gas turbines as above. The model will be divided into two steps that are meshing and steady state thermal analysis. The details of the simulation stage as follows:

Summary of Turbine Blade Geometry

Object Name	<i>9 Holes Turbine Blade</i>
State	Meshed
Definition	
Material	Titanium Alloy
Stiffness Behavior	Flexible
Bounding Box	
Length X	0.1119 m
Length Y	0.14233 m
Length Z	0.201 m
Properties	
Volume	5.1314e-004 m ³
Mass	2.3707 kg
Statistics	
Nodes	40279
Elements	20716

Initial Condition of Analysis

Object Name	<i>Initial Condition</i>
State	Fully Defined
Definition	
Initial Temperature	Uniform Temperature
Initial Temperature Value	1077. °C

Loads Apply on the Turbine blade Model

Object Name	Convection	Convection 2	Convection 3	Convection 4	Convection 5
State	Fully Defined				
Scope					
Scoping Method	Geometry Selection				
Geometry	4 Faces	2 Faces		137 Faces	8 Faces
Definition					
ID	28	29	30	31	32
Type	Convection				
Film Coefficient	3000. W/m ² .°C (ramped)	3000 W/m ² .°C (ramped)	3000. W/m ² .°C (ramped)	1000. W/m ² .°C (ramped)	
Ambient Temperature	1077. °C (ramped)	1077. °C (ramped)	1077. °C (ramped)	327. °C (ramped)	

CHAPTER 4

RESULTS AND DISCUSSION

4.1 Base Model Fluid Flow/External Aerodynamics

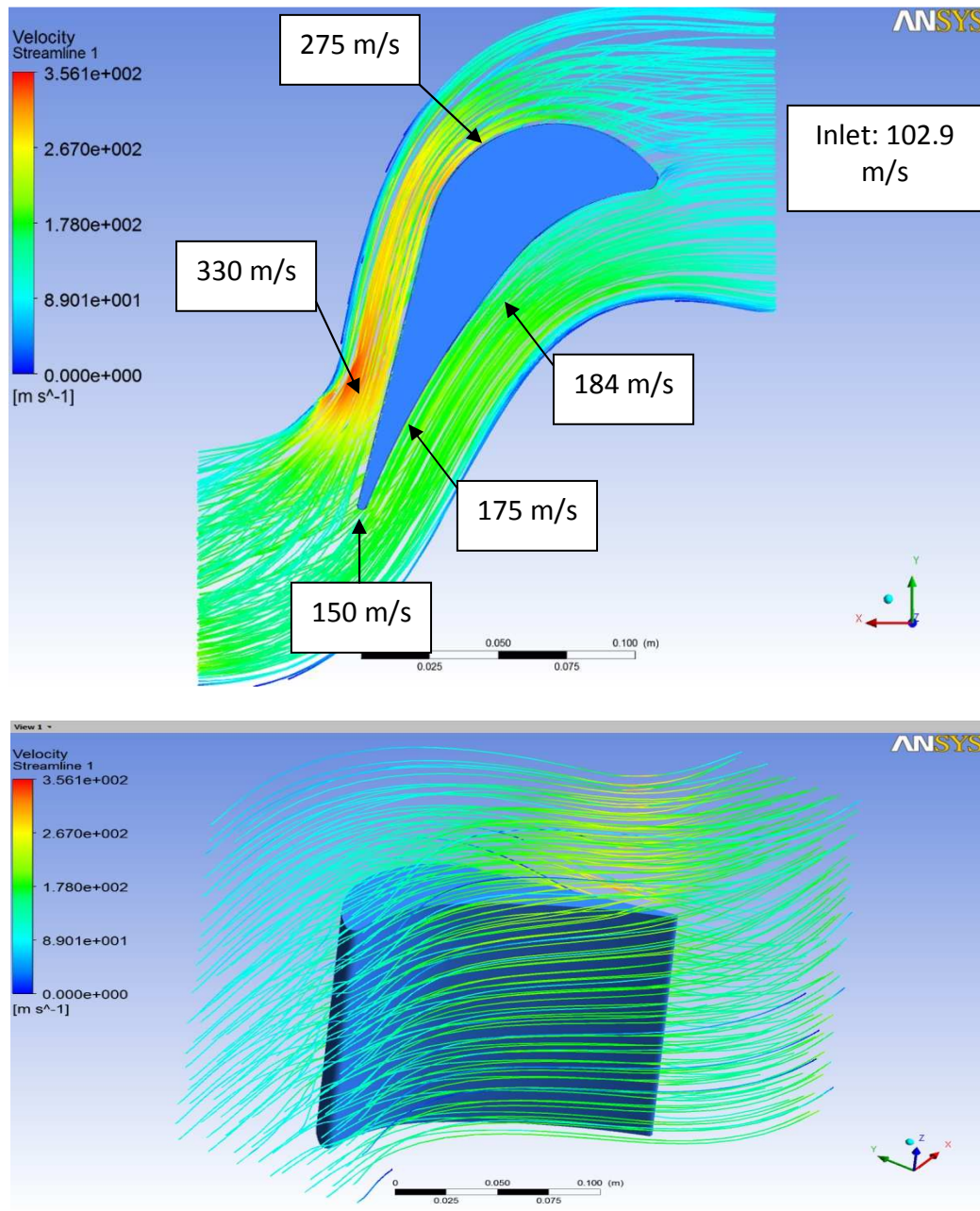


Figure 4.1(a): Fluid flow velocity streamline along the turbine blade model surface

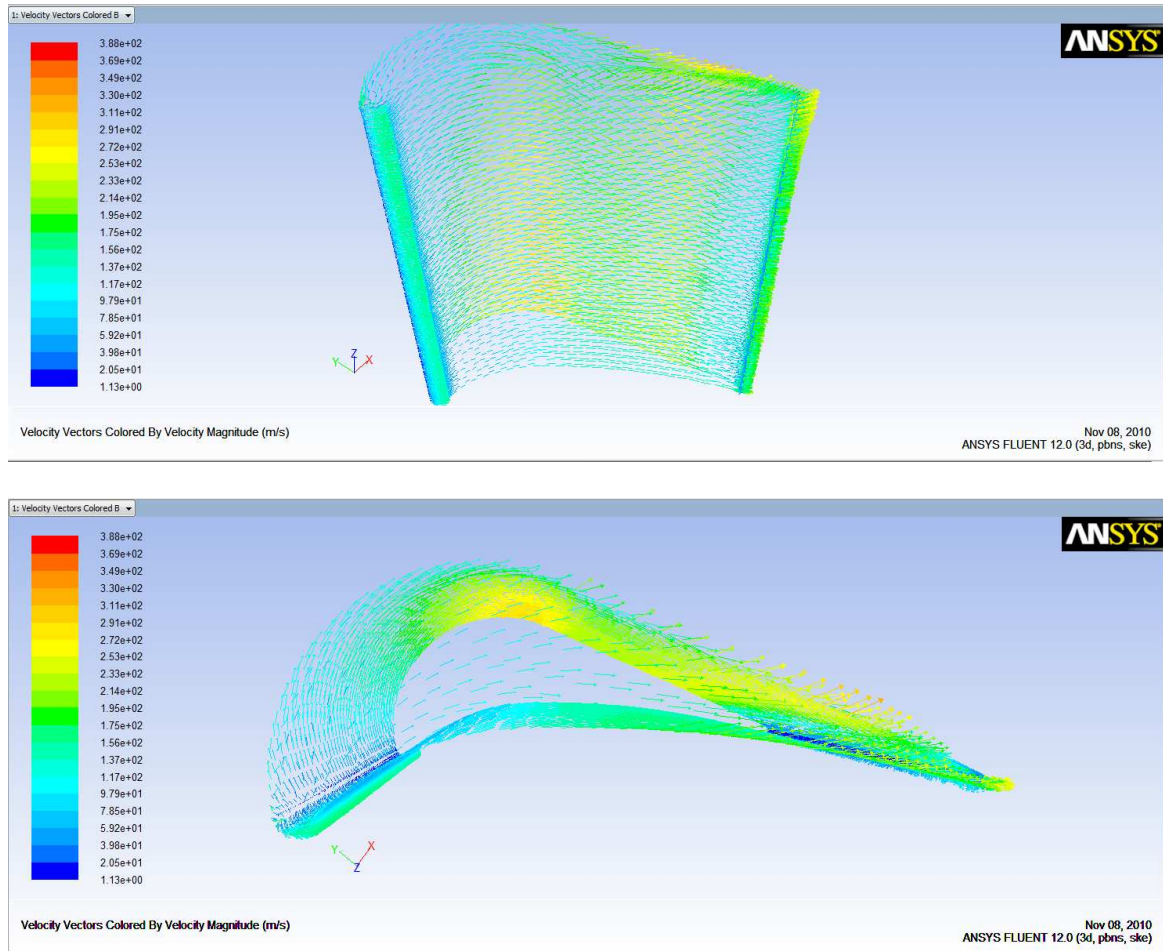


Figure 4.1(b): Fluid flow velocity vectors colored by velocity magnitude of the turbine blade

Computations were performed on the model in the FLUENT based on the boundary conditions and operating conditions from the literature review. Figure 4.1(a) above shows the contours of relative fluid flow velocity streamline along the turbine blade. It represents the fluid particles moving in steady flow. The maximum flow velocity reached about 360 m/s along the passage. The local minimum is on the trailing edge side and leading edge side. The flow velocity after the leading edge side to the trailing side is significantly higher (270-300 m/s and 160-185 m/s approximately). The detail of the flow velocity distribution along the turbine blade is shown in Figure 4.1(b) above. The color contours (fields) represents the range of flow velocity and the arrows the velocity vectors.

4.2 Base Model Temperature Distribution/Thermal Analysis

Figure 4.2 below shows the temperature distribution for the model blade. An important reduction in temperature is observed. The major part of the blade cooling is now performed by the cooling channels. The maximum temperature is observed at the leading edge that is 1022.6°C / 1295.75 K and minimum temperature of the blade is 357.41°C / 630.56 K .

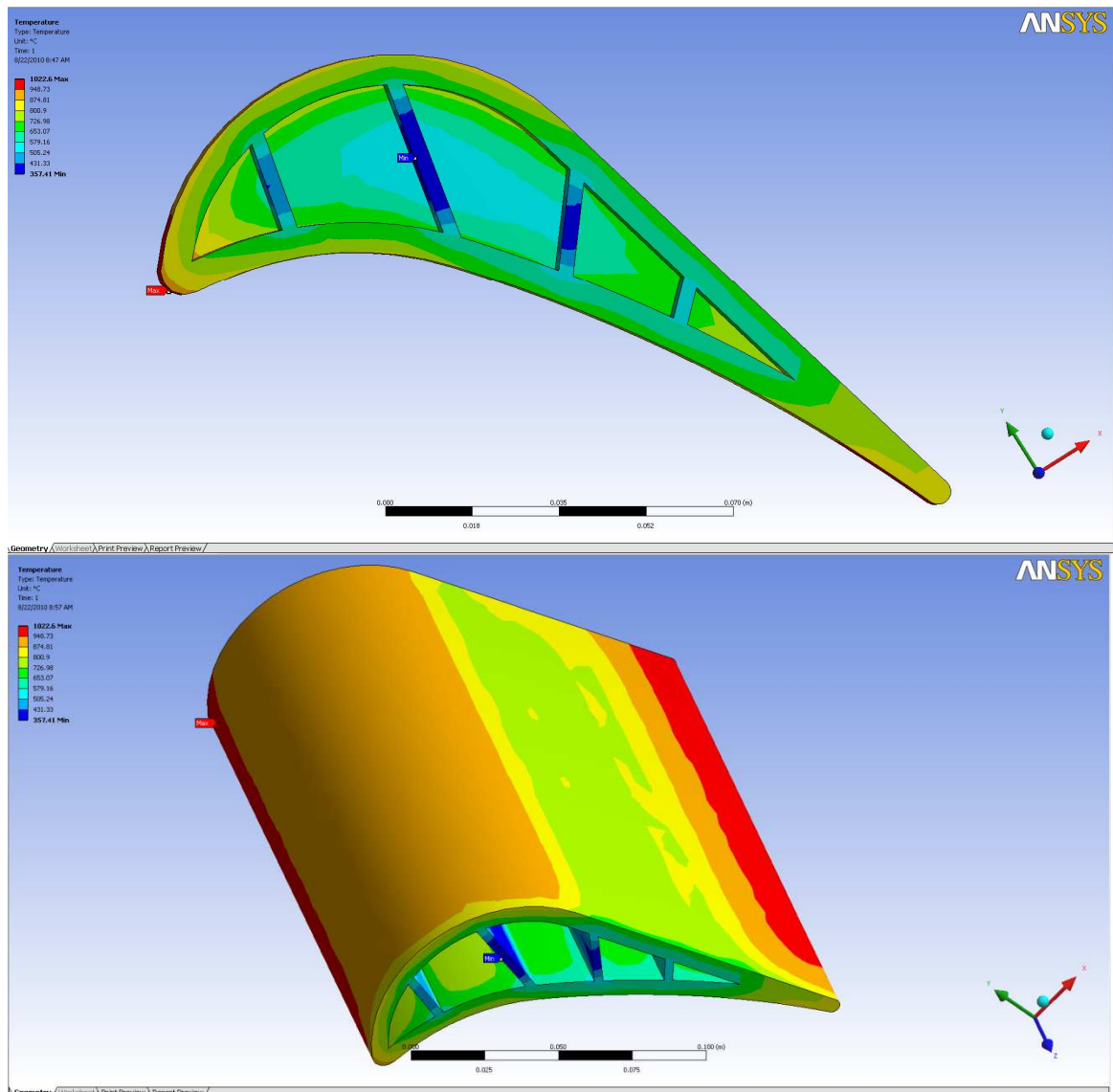


Figure 4.2: Temperature distribution for the blade model

From the simulation and analysis result, the critical parts of the turbine blade are observed at the leading edge and the trailing edge which the average temperature distributions are about 950 °C/1223.15 K. The average temperature distributions are different because of the difference in the convection heat transfer of the fluid (air) along the turbine blade.

The maximum temperature of the material at the blade model is 1022.6 °C / 1295.75 K that is slightly below the maximum operating turbine inlet stage conditions (1077 °C / 1350K) and titanium alloys melting point (~1500 K). So, from the observation, it shows that the internal cooling turbine blade model can control the temperature of the gas turbine to improve engine efficiency by controlling thermal growth. The analysis also proves that the effect of the internal blade cooling can prevent the failure of the turbine blade structure and strength.

By cross referencing the analysis result with the research from Sergio Amaral, Tom Verstraete, Rene Van den Braembussche, Tony Arts, *Design of the Internal Cooling Channels of a High Pressure Turbine Blade : Methodology* Journal [12], it shows that the temperature distribution from both analysis are slightly different. The maximum temperature at the blade from the journal is 1250 K/ 976.85 °C and the analysis result is 1022.6 °C / 1295.75 K which carry out the percentage error of 3-4 %. As the percentage error from the analysis and the journal is small (<5%), the result of the analysis is valid and comparable.

However, the maximum temperature at the turbine blade are not as expected and quite different. The journal shows the maximum temperature of the blade model is at the trailing edge tip and from the analysis result, the maximum temperature of the model is at the leading edge. The difference of the results may caused by several aspects.

Firstly, the differentiation of the geometry and dimensions of the turbine blade affect the results. Secondly, the dimensions on the internal cooling channel of both model is not the same. As the analysis result proves that the cooling blade model can prevent from failure, this turbine blade model will be made as the base model for the author. Furthermore, table below shows the summary of the analysis result.

Results Summary

Object Name	<i>Temperature</i>
Scope	
Geometry	All Bodies
Definition	
Type	Temperature
Display Time	End Time
Results	
Minimum	357.41 °C
Maximum	1022.6 °C

4.3 Turbine Blade Model with External and Pin-Fin Holes

As for the sensitivity study stage, the impact of the analysis and simulation results for different designs is assessed by comparing the results of a blade without external and pin-fin holes with the ones of a blade where the cooling channels are evenly distributed along the camber line with external and pin-fin holes.

Figure 4.3 below shows the temperature distribution for the blade with external and pin-fin cooling holes. An important reduction in temperature is observed. The major part of the blade cooling is now performed by the cooling channels and the flow in external and pin-fin cooling holes that has small impact on the cooling. The maximum material temperature, again observed at the leading edge, is reduced to 1019.3 °C /1292.45 K.

Even though the difference of the temperature is slightly small, but the holes improve the convection heat transfer on the trailing edge of the turbine blade model. The average of the temperature distributions at the trailing edge now is reduced from 950 °C/1223.15 K to 820 °C/ 1093.15 K which about 15% of reduction.

From the analysis, it proves that the effect of the external and pin fin holes is critical for the turbine blade to reduce the temperature distribution along the blade especially at the trailing edge. The trailing edge at the blade is critical because of the maximum convective heat transfer for the fluid flow instead of the leading edge. So, these external and pin-fin cooling holes will further improve the engine efficiency by controlling thermal growth better and increase the possibility to prevent the blade from failure. The summary of the analysis results for the turbine blade design as per table below.

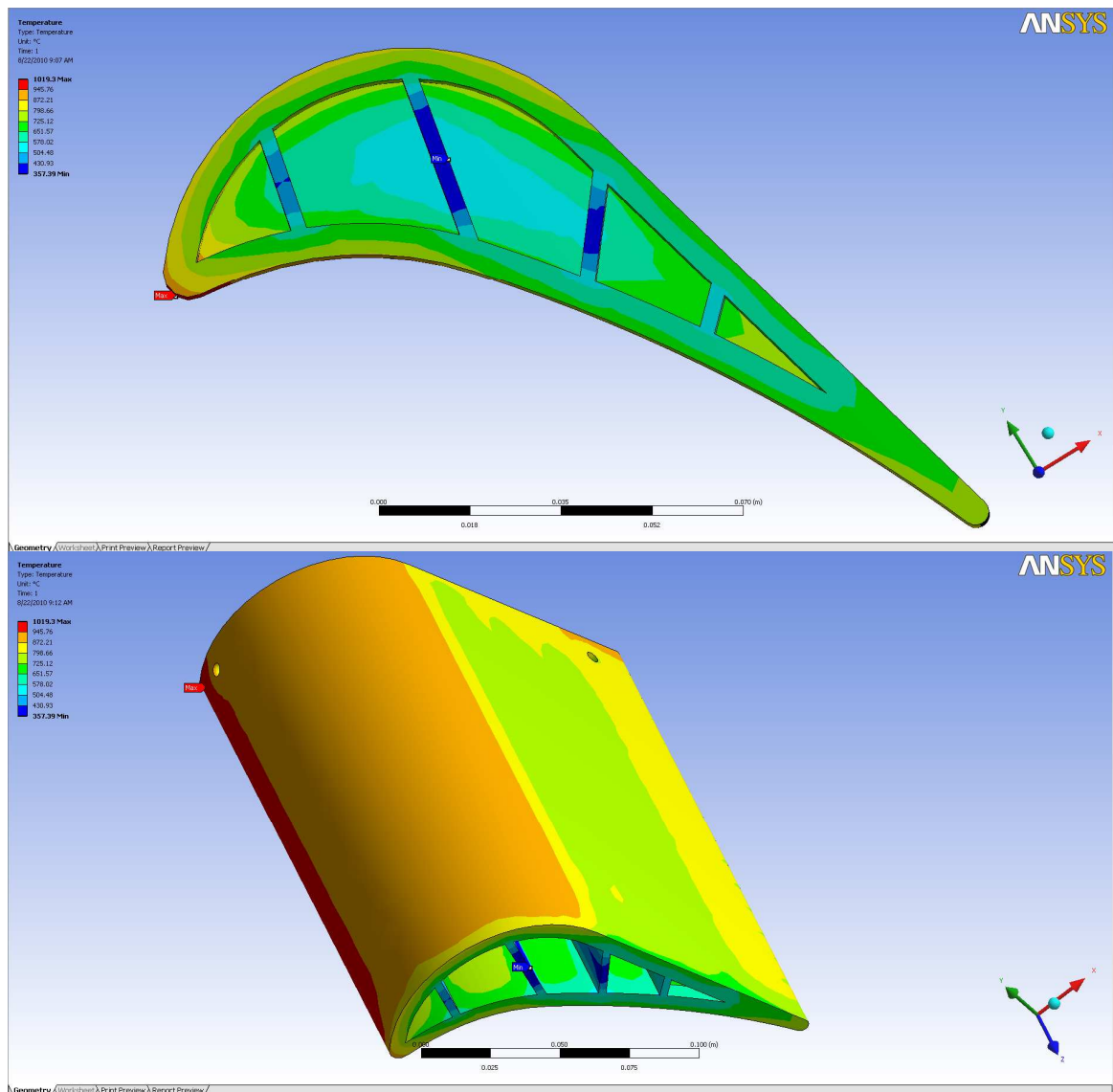


Figure 4.3: Temperature distribution for the blade model with external and pin-fin holes

Results Summary

Object Name	Temperature
Scope	
Geometry	All Bodies
Definition	
Type	Temperature
Display Time	End Time
Results	
Minimum	357.39 °C
Maximum	1019.3 °C

4.4 Turbine Blade Model with 9 Cooling Channels

Then, the impact of the analysis and simulation results for different designs is assessed by comparing the results of a blade with different numbers of cooling channels that is 9 cooling channels instead of 5 cooling channels from base model. The design geometry of the model is based on the geometry from the journal as Figure 12 above [13].

Figure 4.4 below shows the temperature distribution for the blade with 9 cooling holes. An important reduction in temperature is observed. The major part of the blade cooling is now performed by the 9 cooling channels. The maximum material temperature, again observed at the leading edge, is reduced to 1021.7 °C /1294.7 K.

Even though the difference of the temperature is slightly small, but the different number of channels improves the convection heat transfer on the trailing edge of the turbine blade model. The average of the temperature distributions at the trailing edge now is reduced from 950 °C/1223.15 K to 800 °C/ 1073 K which about 19% of reduction. The average temperature distribution of the overall turbine blade wall is also decreased and improved.

From the analysis, it proves that the affect of the different number of cooling channels is critical for the turbine blade to reduce the temperature distribution at along the blade. So, these 9 cooling channels will more improve the engine efficiency by controlling thermal growth better and increase the possibility to prevent the blade from failure. The summary of the analysis results for the turbine blade design as per table below.

Results Summary	
Object Name	<i>Temperature</i>
State	Solved
Scope	
Geometry	All Bodies
Results	
Minimum	345.58 °C
Maximum	1021.7 °C

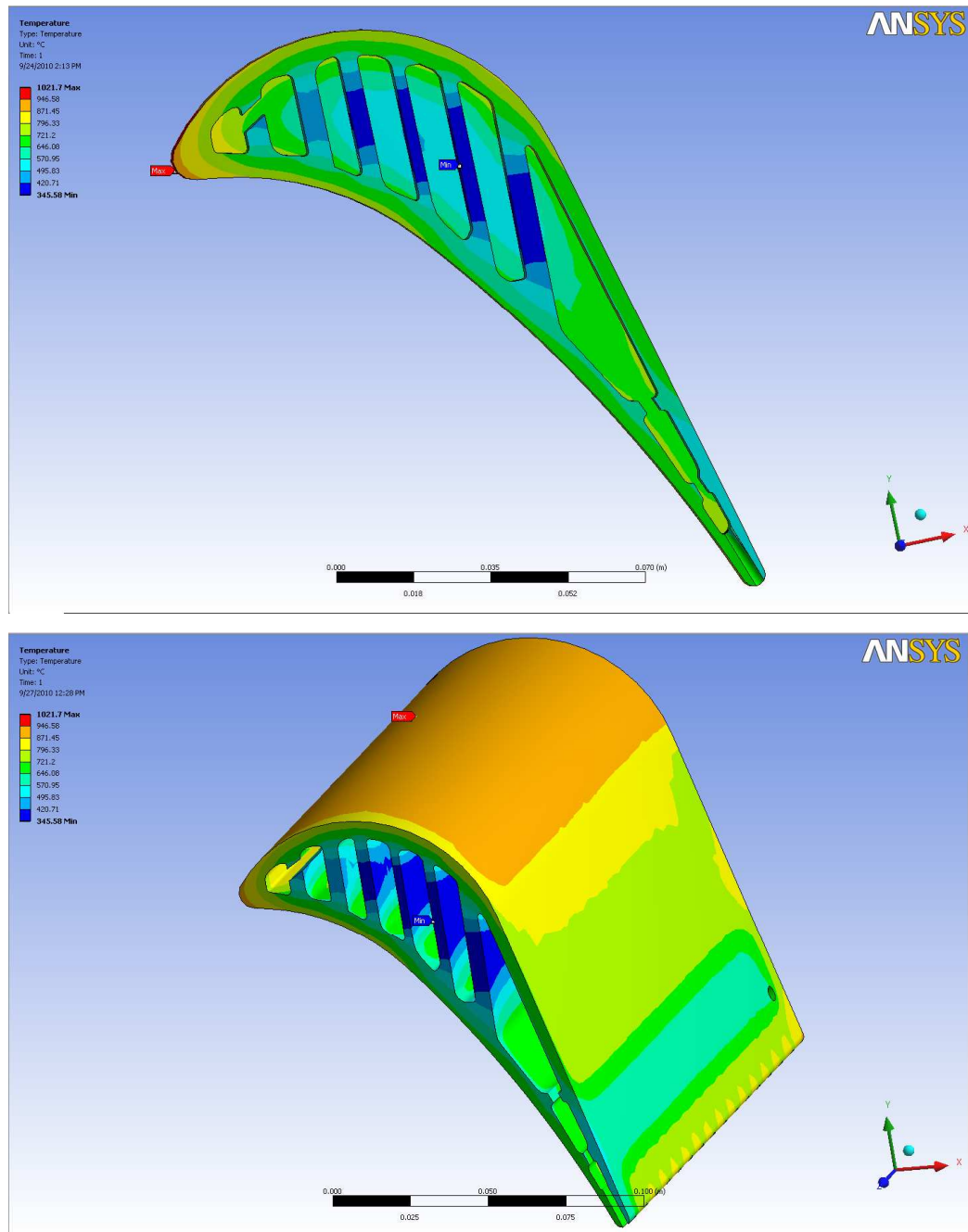


Figure 4.4: Temperature distribution for the blade model with 9 cooling channels

CHAPTER 5

CONCLUSION

As conclusion, the reasons of the gas turbine internal cooling blade study are to investigate the temperature profile along the surface and to study on the thermal analysis on the temperature distributions along the turbine blade. The importance of the analysis is to help the author in designing efficient cooling system. The fluid flow velocity and linear steady-state thermal analysis has been made and the result shows the blade model can be made as the based model as it proves that the model can prevent the blade from thermal failure. As the base turbine blade model design and the analysis meet the specification, the sensitivity study has been carried out. The objective of this sensitivity study is to observe for the change in the result of the thermal analysis of the turbine blade when one of the parameter designs change. As examples, the effect of the number, sizes and types of holes at the turbine blade. Firstly, the author observes on the change of the design blade with the external holes and pin-fin cooling holes. From the simulation and analysis, it is proves that the design with holes slightly affect the temperature distribution along the turbine blade. The major impact of the design is observed at the trailing edge of the blade which gives the difference of 15% reduction. Then, the author observes on the effect of the number of holes with 9 cooling channels. From both of the sensitivity study, the results show the holes at the blade and increase of number of cooling channels will improve the efficiency of the engine better as the thermal growth along the blade is improved.

REFERENCES

- [1] Je-Chin Han, Sandip Kutta, and Srinath V. Ekkad, 2000, *Gas Turbine Heat Transfer and Cooling Technology*.
- [2] HHH Saravanamuttoo, GFC Rogers, H Cohen, PV Straznicky, Sixth Edition, 2009, *Gas Turbine Theory*.
- [3] Halila, E.E., Lenahan, D.T., and Thomas, T.T., 1982. *Energy Efficient Engine*.
General Electric Company (prepared for NASA CR-167955)
- [4] Gladden, H.J., and Simoneau, R.J., 1988, "Review and Assessment of the Database and Numerical Modeling for Turbine Heat Transfer." In *Toward Improved Durability in Advanced Aircraft Engine Hot Sections*. Edited by D.E Sokolowski
- [5] Han, J.C. and Dutta, S., 1995. *Internal Convection Heat Transfer and Cooling: An Experimental Approach*.
- [6] Lakshminarayana, B., 1996. "Turbine Cooling and Heat Transfer." In *Fluid Dynamics and Heat Transfer of Turbomachinery*.
- [7] J.H. Horlock and L. Torbidoni, 2006, *Turbine Blade Cooling: The blade Temperature Distribution*.
- [8] U. Uysal, P. Li, M.K. Chyu, and F.J. Cunha, 2006 "Heat Transfer on Internal Surfaces of a Duct Subjected to Impingement of a Jet Array with Varying Jet Hole-Size and Spacing," ASME GT2005-68944, *Trans. ASME Journal of Turbo machinery*.
- [9] R. Gardon and J. Cohonpue, 13, 1977. "Heat Transfer Between a Flat Plate and Jet Air Impinging on It," ASME/AICHE International Heat Transfer Conference Proceedings, 1962; H. Martin, "Heat and Mass Transfer Between Impingement Gas Jets and Solid Surfaces," *Advances in Heat Transfer*.
- [10] Frank J. Cunha, Ph.D., P.E, *Heat Transfer Analysis Journal*.
- [11] A. Yangyozov, R. Willinger, *Journal on Calculation of Flow Characteristics in Heat Turbo machinery Turbine Stage with Different Three Dimensional Shape Of the Stator and Rotor Blade with ANSYS CFX Software*.
- [12] Sergio Amaral, Tom Verstraete, Rene Van den Braembussche, Tony Arts, *Design of the Internal Cooling Channe;s of a High Pressure Turbine Blade : Methodology*
- [13] W.B. de Wolf, S. Woldendorp and T. Tinga, *Analysis of the combined Convective and film cooling on an existing turbine blade*

APPENDICES

APPENDIX I – An overall view of the rotor, stator, and casing cooling supply system for E³ Engine (Halila e al.,1982, NASA CR-167955)

APPENDIX II – Cooling and Sealing Air System of the Rolls Royce RB211-24G

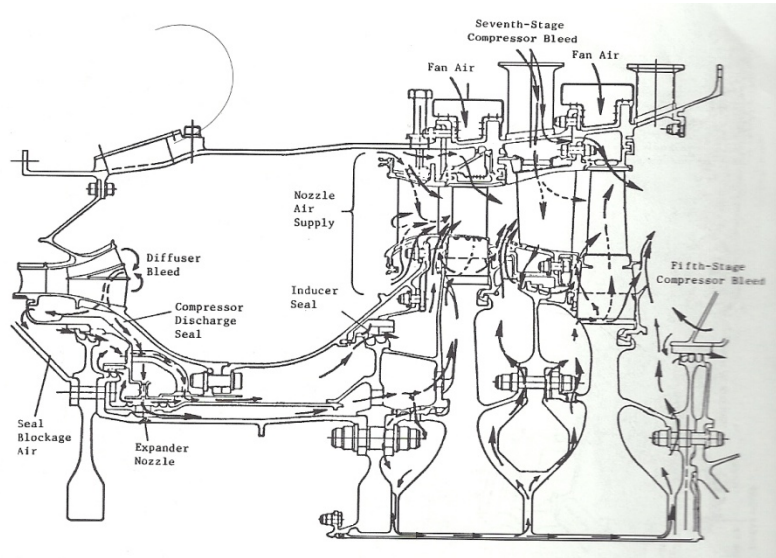
APPENDIX III – Gas Turbine Internal Cooling Blade Model

APPENDIX IV – Gas Turbine Internal Cooling Blade Model with External Holes and Pin-Fin Cooling Holes

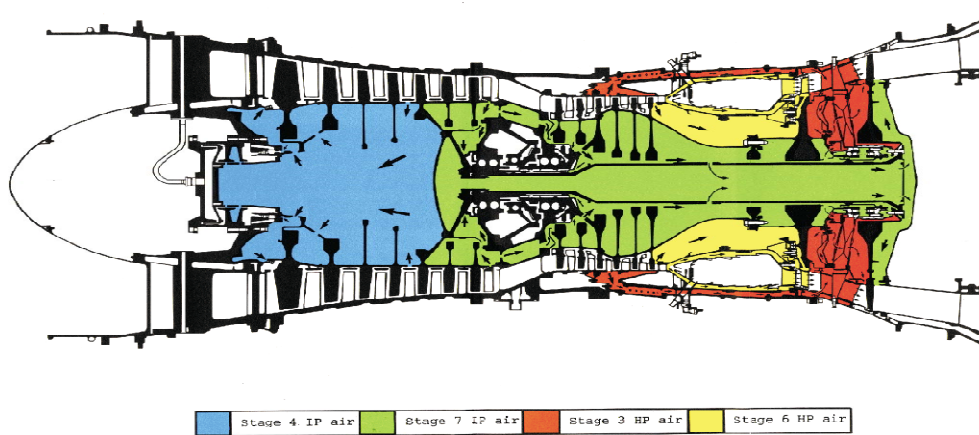
APPENDIX V – Temperature Distribution of the Blade Model

APPENDIX VI – Temperature Distribution of the Blade Model with External holes and Pin-Fin Cooling Holes

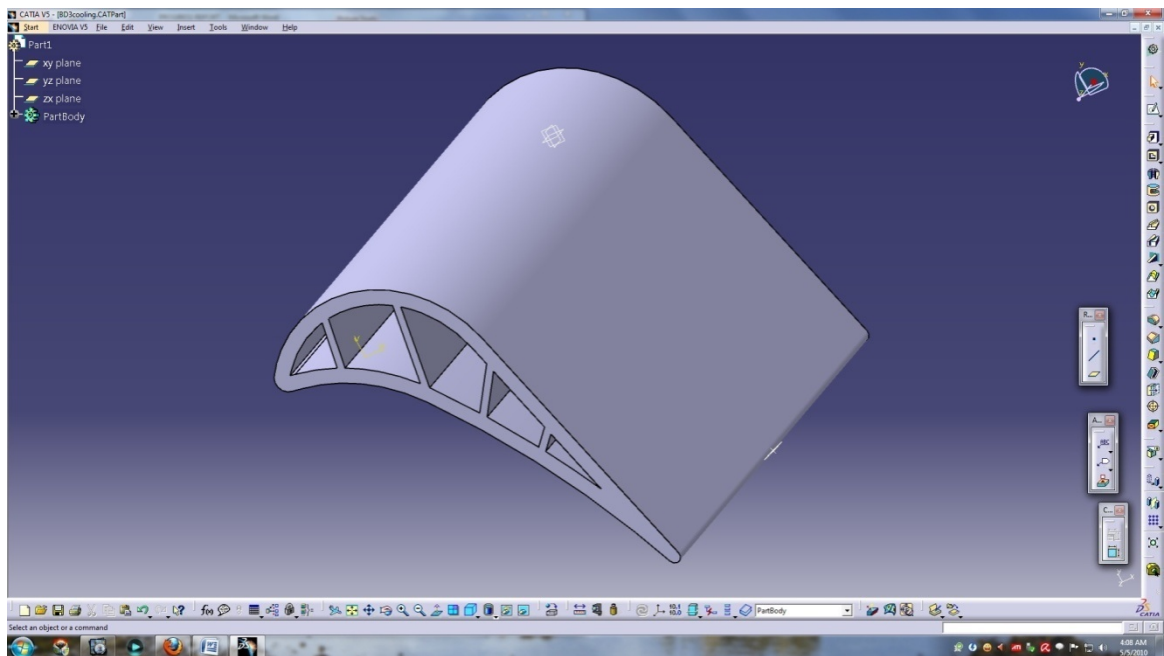
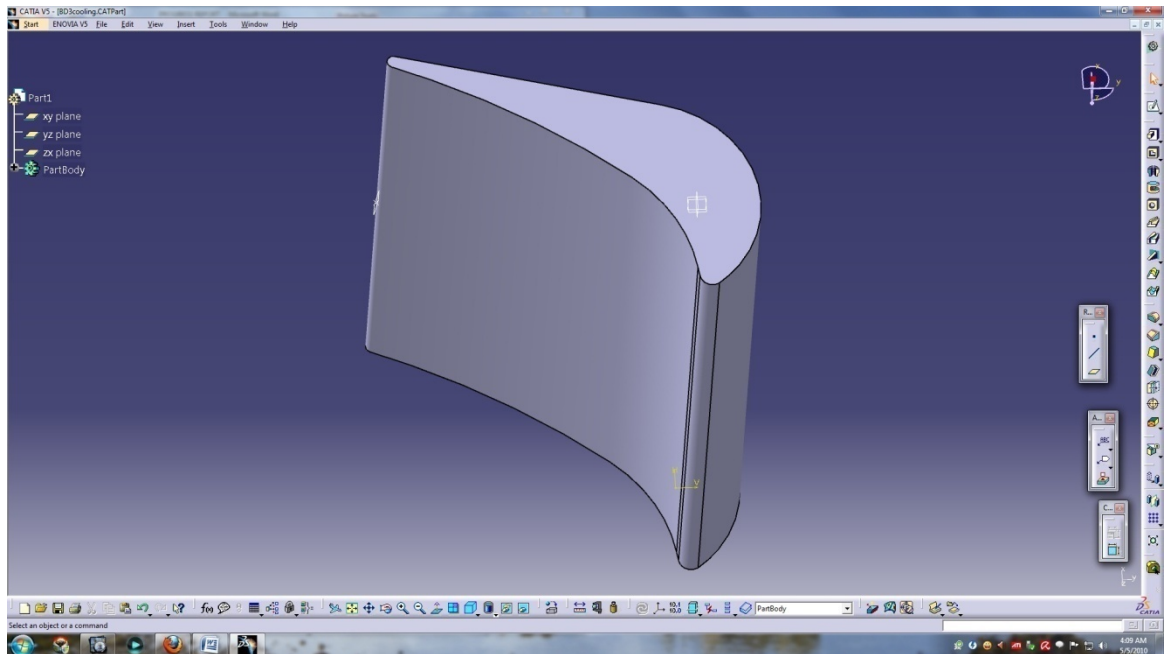
APPENDIX I: An overall view of the rotor, stator, and casing cooling supply system for E³ Engine (Halila e al.,1982, NASA CR-167955)



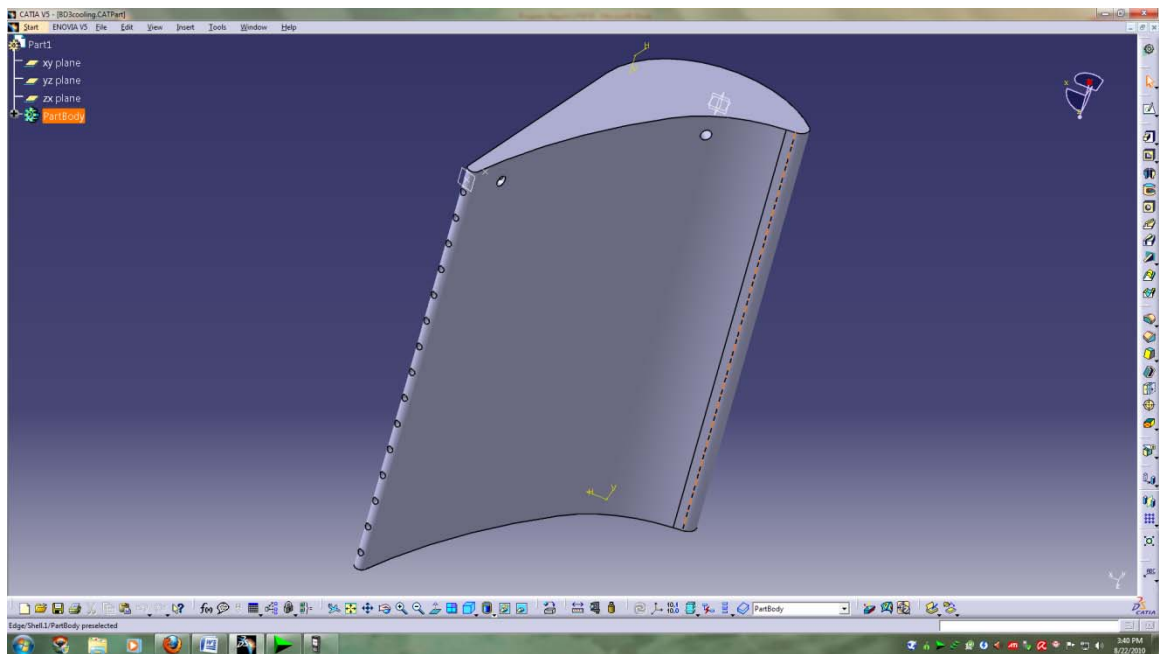
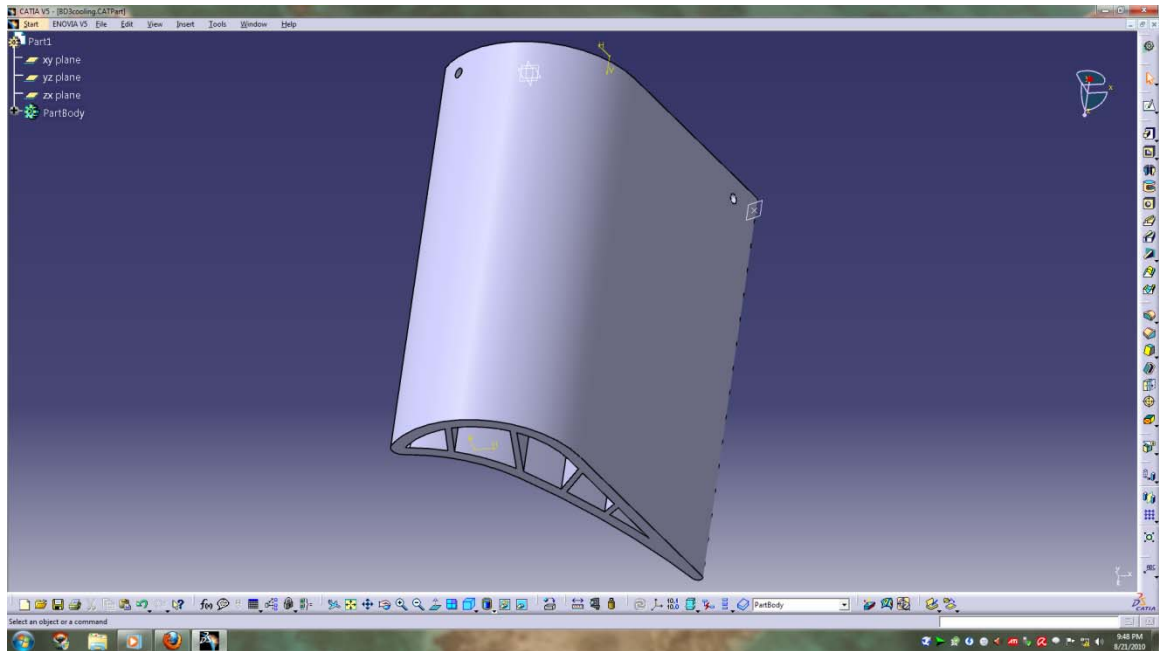
APPENDIX II: Cooling and Sealing Air System of the Rolls Royce RB211-24G



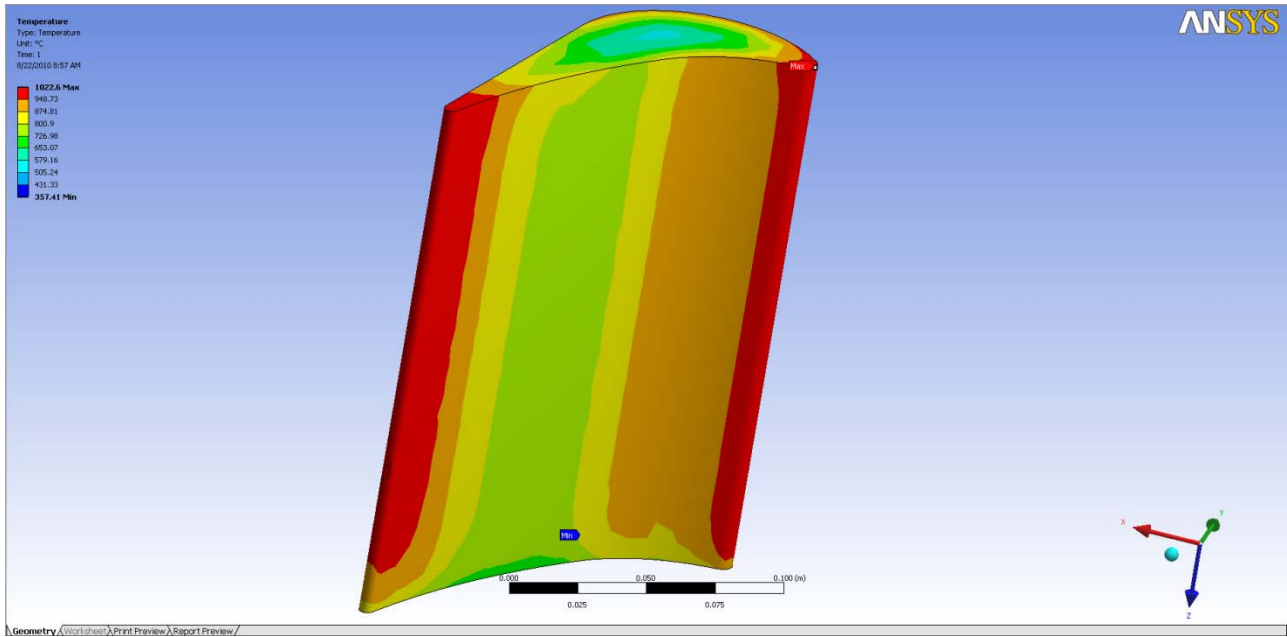
APPENDIX III – Gas Turbine Internal Cooling Blade Model



APPENDIX IV – Gas Turbine Internal Cooling Blade Model Model with External Holes and Pin-Fin Cooling Holes



APPENDIX V – Temperature Distribution of the Blade Model



APPENDIX VI – Temperature Distribution of the Blade Model

